Laboratory For Atmospheric And Space Physics

LASP Mission Operations and Data Systems Division

University of Colorado

Boulder, Colorado

EUV Variability Experiment
(EVE)
Ground Spectra Measurements

Document No. EVE-S-87099 Rev. 2 (draft) Date: 09/18/07

Revisions

Rev	Description of Change	By	Approved	Date
1	1st draft	D. Woodraska	N/A	09/18/07
2	2nd draft – added flatfield intensities	D. Woodraska	N/A	05/22/08

Prepared by _Donald L. Woodraska, Ph.D._____ Date _09/18/07_
EVE Science Data Processing Lead

1. Purpose and Scope

This document captures the current state of understanding of the ground calibration performed at the Laboratory for Atmospheric and Space Physics (LASP) for the Extreme Ultraviolet Variability (EUV) Experiment (EVE), which is one instrument on the Solar Dynamics Observatory (SDO). SDO is scheduled to launch in January 2009 into a geosynchronous orbit to perform nearly continuous observation of the sun. EVE is required to perform spectral measurement of the solar EUV at a cadence of at least 20 seconds (plan is 10 seconds) for at least 90% of the time. EVE performs spectral measurements with a pair of Multiple EUV Grating Spectrographs (MEGS) 2048x1024 CCDs, namely MEGS-A and MEGS-B. MEGS-A spans approximately 5-37 nm and MEGS-B spans approximately 35-105 nm which provides a slight overlap in the two channels. Further details are recorded in other documents (ref. Crotser, et al. 2007, Triplet, et al 2007, Eparvier, et al. 2003). This document does not describe any of the photometer measurements or calibration.

All spectra were measured from a hollow cathode (HC) lamp built by LASP. The HC lamp uses high voltage (several kV) to excite and ionize an unconfined flow of a source gas. The excited gas (plasma) then releases energy through electronic emission (and other processes such as collisions). The gas flow rate and voltage are tuned to reduce self-absorption and increase emission for most gases. All measurements were collected in the MOBI vacuum chamber in the LASP Space Technology Building in Boulder, CO.

2. MEGS-A

Several gases were used to determine optical performance and verify the alignment of MEGS-A grating relative to the optical reference defined by the Solar Aspect Monitor (SAM). MEGS-A has two optical paths, and only the top half could be used due to calibration source emission limitations.

2.1 Helium

The entire wavelength range for MEGS-A is shown in Figure 1 with Helium (He) measurements. Vertical stripes represent specific atomic emissions in He and He+. This image has been greatly contrast enhanced, but has not been dark corrected. The spectrum for Helium is shown with long wavelengths on the left, and short wavelengths towards the right. The lower portion shows a dark vertical stripe indicative of non-uniformities in the thermally-generated electrons in the silicon wafer.

The top portion is where the spectrum falls. The left-most edge shows elevated thermal signatures that do not span completely across the top-half.

Moving to the right, the spectral lines are seen with the intensity dictating the apparent vertical height of the lines. The brightest line (also tallest) is the He II 30.378 nm line, corresponding to emission from the first excited state down to the ground state (n=2 to n=1). Weak lines surrounding this line are likely impurities in the source gas, or extraneous emission due to the particulars of the HC lamp with this specific high voltage setting and flow rate. These parameters

were tuned to brighten the known dimmer lines. Further to the right are several other well-known lines including 24.303, 23.733, 23.435 nm, and others. These terminate near 22.864 nm corresponding to the theoretical Rydberg transition from n=15 to n=1.

Just to the right of the highest Rydberg transition detectable is another feature which is believed to be caused by a dust particle on this particular filter. Another filter will be used as the primary science filter. This is believed to be a particle because it moves when the filter wheel is stepped (detected at NIST-SURF, not shown).

Further towards the right starting near the middle of the top-half of the detector, a noticeable intensity ramp-up is detectable. "This feature is visible light diffraction from the entrance slit imaged at the detector. Due to imaging aberrations, highly off-axis diffracted light is not perfectly imaged into 0th order and therefore appears in the short-wavelength spectral region of the detector." This is diffracted light being clipped by the 0^{th} order baffled edge near pixel 800. This diffraction effect can be modeled and removed. This experimentally measured using 2 different wavelength lasers which produced different diffraction patterns (not shown).

Near the right edge of the detector a slightly brighter, but very diffuse line-like shape is noticeable (glint). This occurs at a wavelength that is believed to be outside the required science range. "This feature is an aberrated visible light image of an off-axis (-4 degrees) baffle edge glint." This shape does not move horizontally like the spectral lines do, so it is not being imaged by the grating.

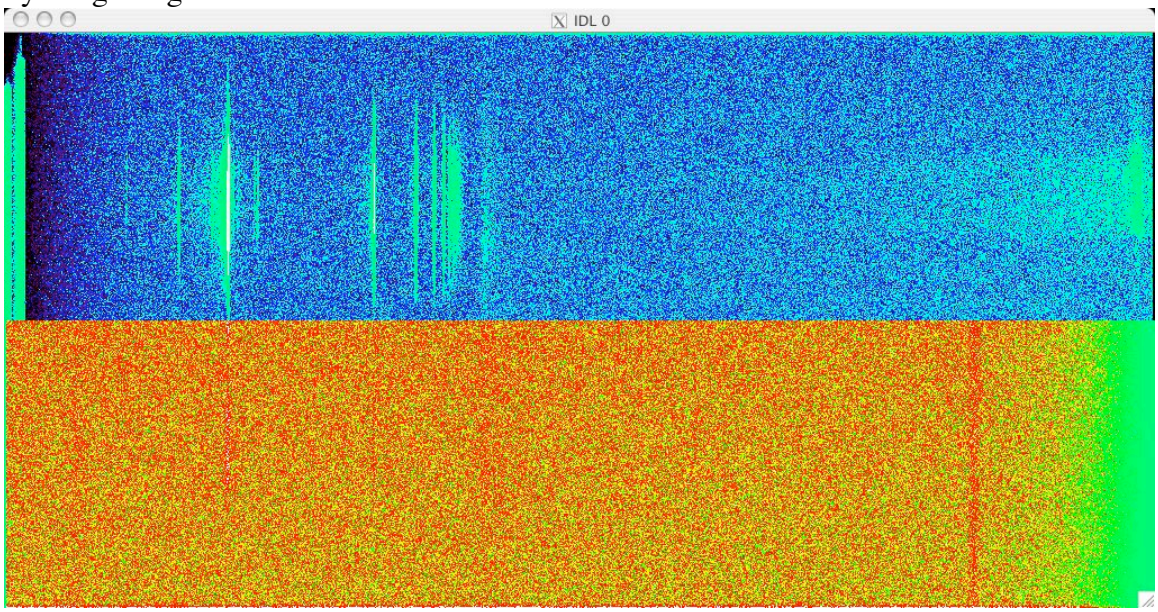

Figure 1. MEGS-A image of Helium.

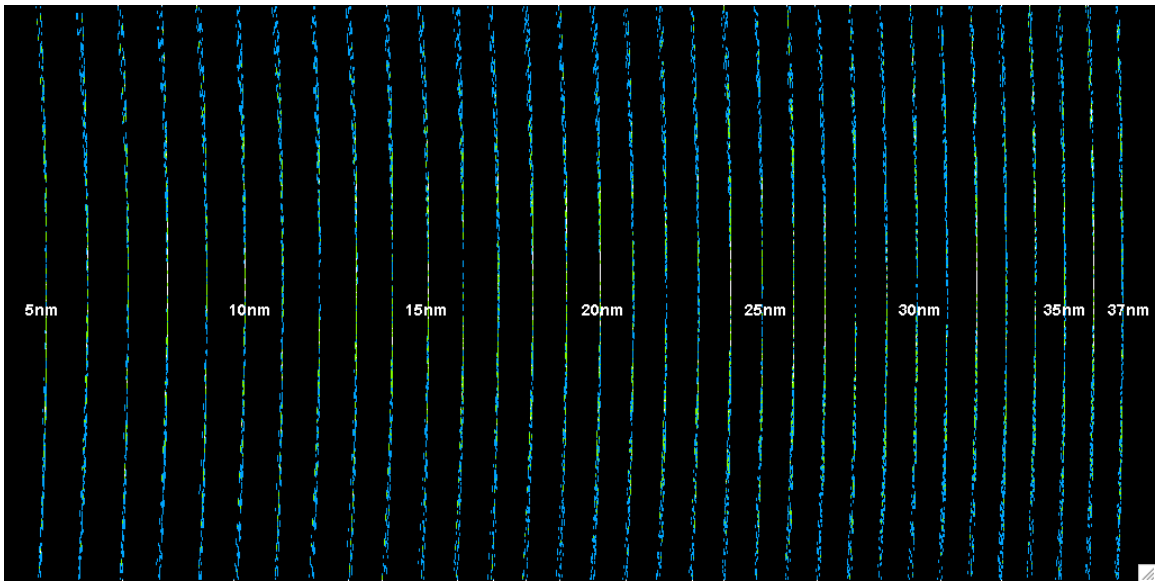

Figure 2. Ray-trace result for a nominal pointing wavelength scale (Crotser) with slit divider removed, all lines are somewhat curved.

From Figure 1 we can create a spectrum as shown in Figure 3, Figure 4, Figure 5, and Figure 6.

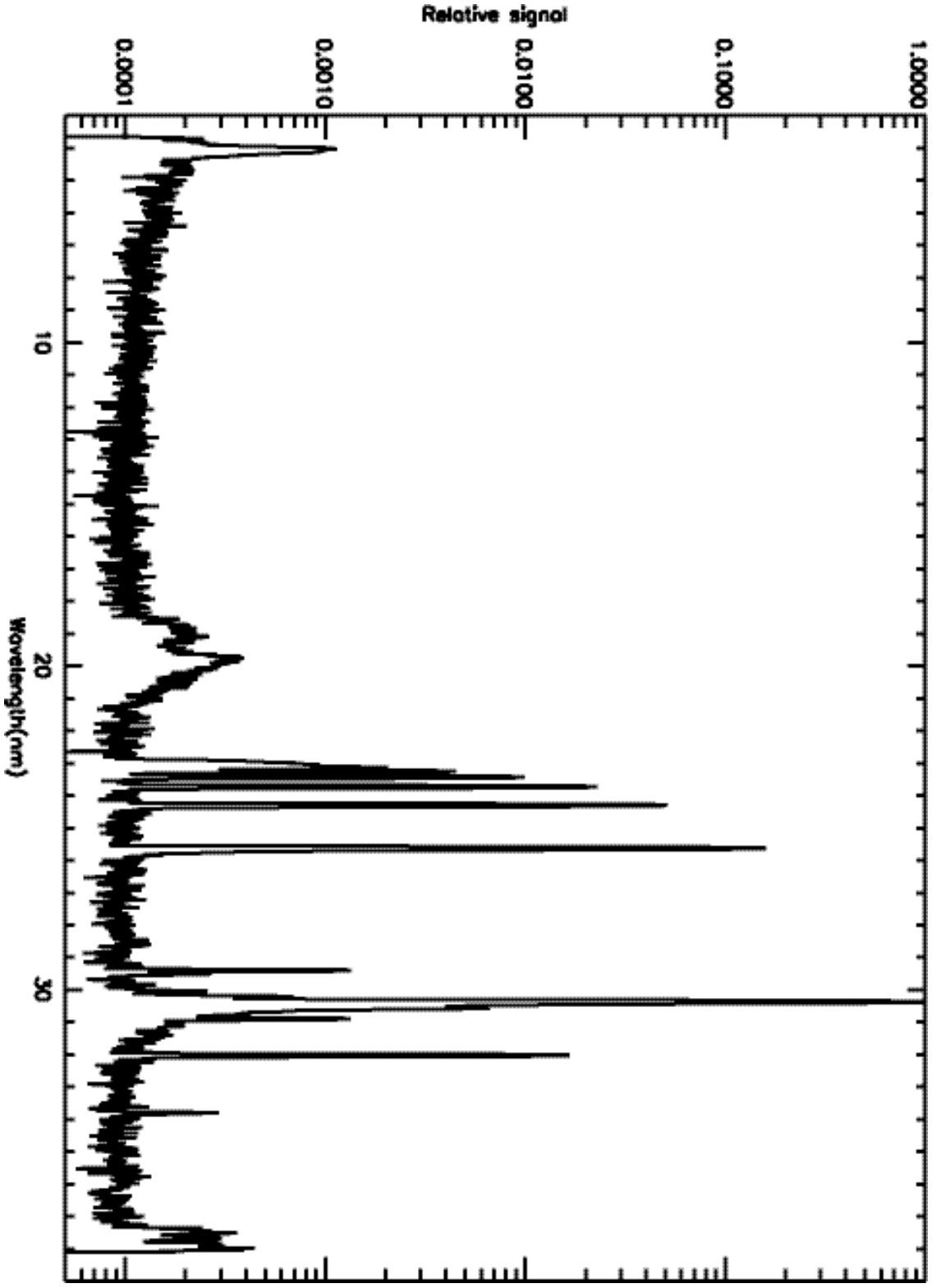

Figure 3. MEGS-A slit 2 (top) Helium spectrum with wavelength scale.

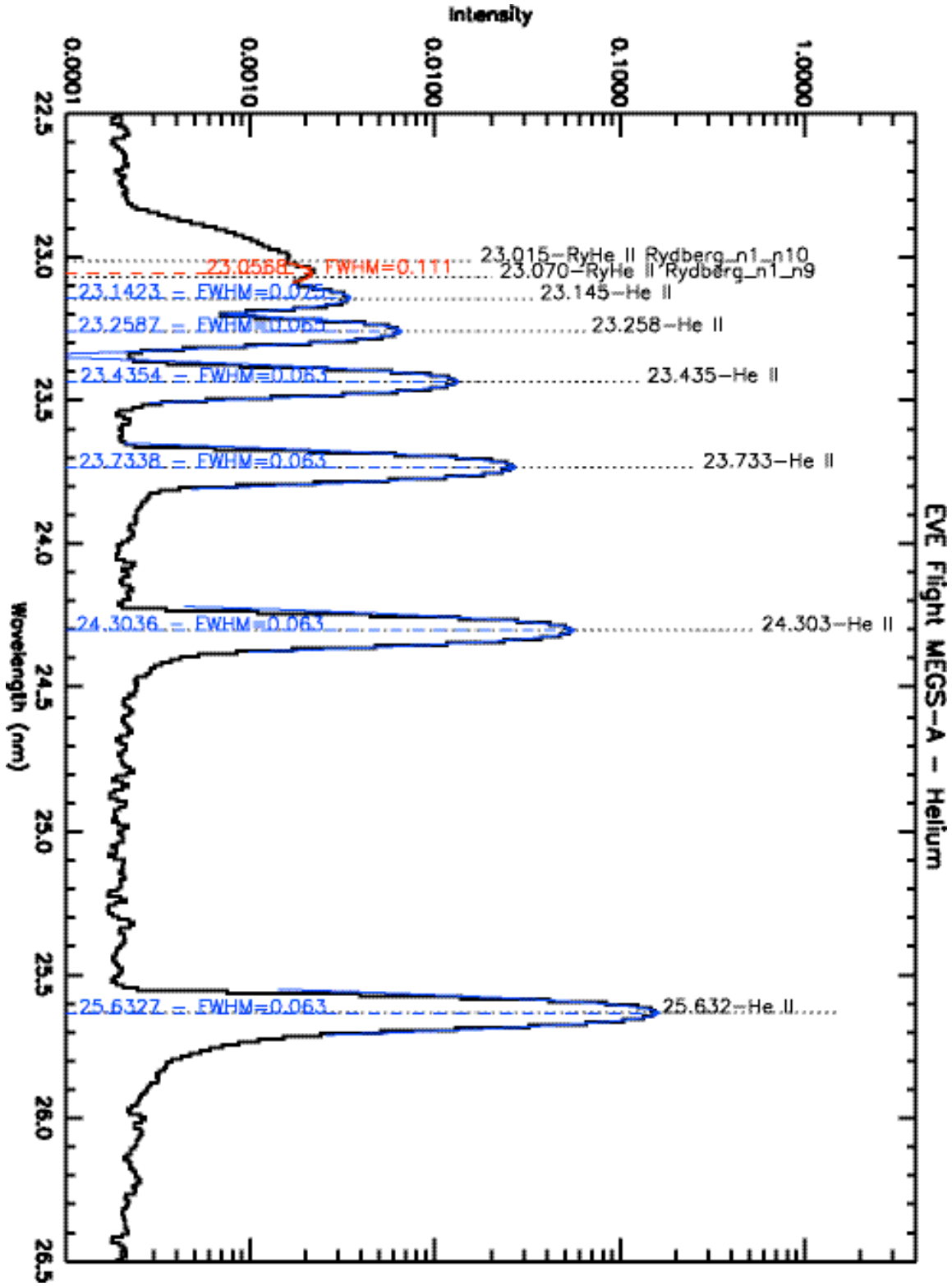

Figure 4. MEGS-A partial Helium spectrum part 1 with spectral line identifications and resolution achieved.

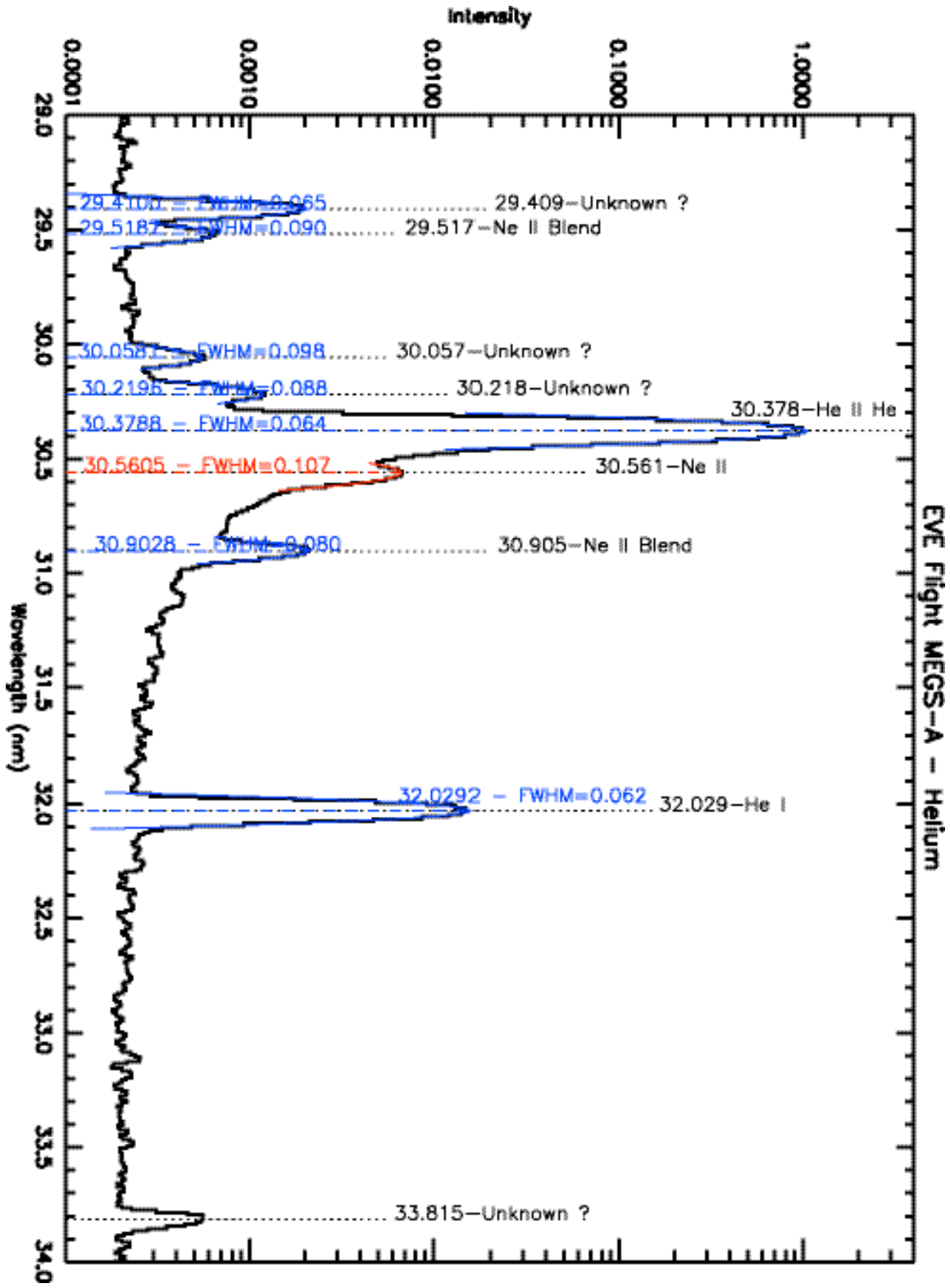

Figure 5. MEGS-A partial Helium part 2 with spectral line identifications and resolution achieved.

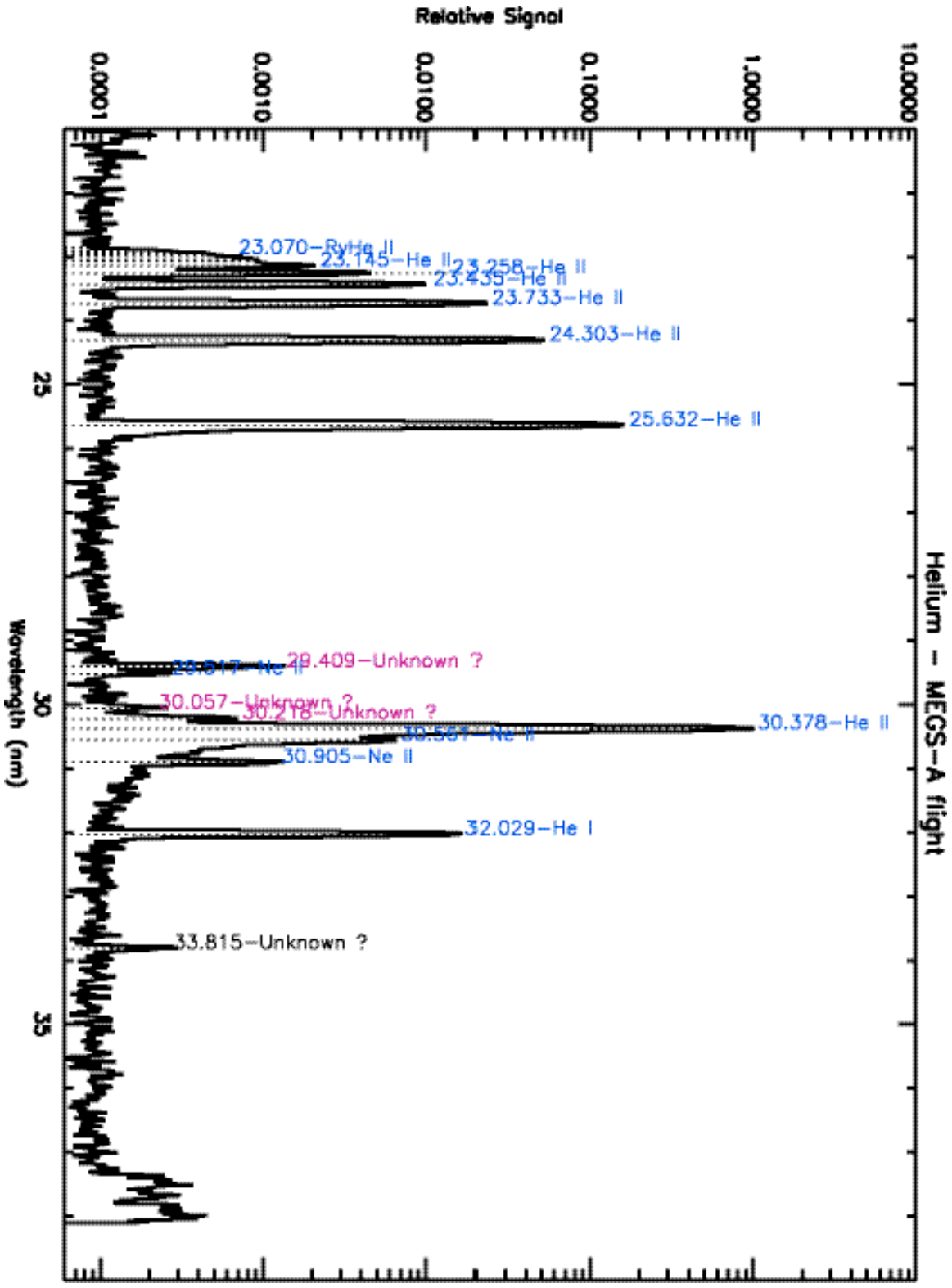

Figure 6. MEGS-A complete helium line spectrum from 25 minutes.

The figures were generated with differing numbers of integrations, so background subtraction is different, thus the noise floor is varying. Note that not all lines have been identified, but all known Helium lines are labeled. Certain lines are residual gases from previous measurements and slowly decay. Selected lines have been fitted to a Gaussian (which is not the correct profile) in order to provide a quantifiable estimate of the resolution (full width at half-max FWHM). Most lines have FWHM in the range of 0.063 nm, and those that do not are likely blended. MEGS-A exceeds the design requirement of 0.1 nm for the portion that is illuminated by the HC lamp.

The spectra are generated in bins of 0.01 nm (level 1) which is useful for detector characterization. However, the level 2 public product will be at 0.05 nm to maintain full instrument resolution while minimizing download sizes, and provide a consistent wavelength scale with the other CCD detector, MEGS-B.

2.2 Neon

Although Helium provides easily identifiable lines, the actual wavelength coverage is not complete. Over half the detector has no lines for Helium. In order to increase the wavelength coverage, we measured Neon as well.

A neon spectrum with many lines is shown in Figure 7. The diamonds represent the FWHM from Gaussian fits to the lines which are mostly consistent with the Helium results. Neon has emission lines that are shorter wavelength then the Helium II continuum (near 22.7 nm), and also more lines all the way up to the overlap region with MEGS-B. The greatly enhances the constraints for wavelength scale fitting.

The neon spectrum is littered with lines but we require fairly evenly distributed isolated lines to perform the wavelength scale fitting. This is particularly problematic for extrapolating the wavelength scale toward shorter wavelengths. The best wavelength scale was determined using both the Helium and Neon spectra. The ray-trace model results were adjusted to match the measured lines, and then the model was used the regions where no lines could be measured.

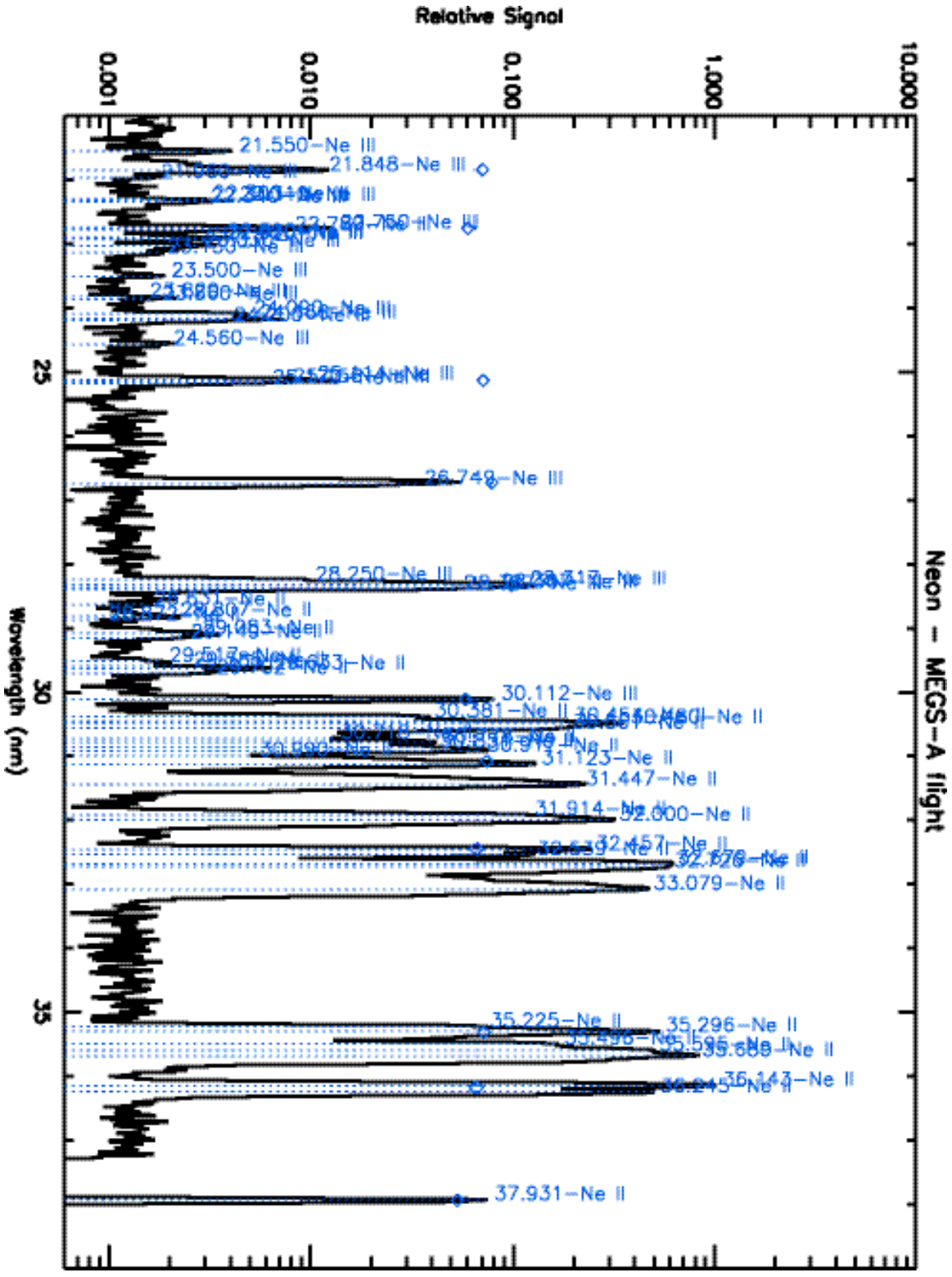

Figure 7. MEGS-A Neon spectrum.

2.3 Other sources

No other line sources produced lines on MEGS-A. We tried N_2 and Ar which produced lines in MEGS-B.

We also tried using a "Manson source" to observe shorter wavelengths to no avail. The two targets tried were Al and MgO. Despite being observed with SAM and ESP, these produced no photons with wavelengths longer than 5 nm.

3. MEGS-B

Several gases were used to determine optical performance and verify the alignment of MEGS-B gratings and intermediate slit/baffle relative to the optical reference defined by the Solar Aspect Monitor (SAM). MEGS-B has two cross-dispersed gratings so the spectra lie along a nearly diagonal curve spanning the top and bottom halves.

3.1 Helium

A sample image of the Helium spectrum is shown in Figure 8. Short wavelengths are located on the left, and longer wavelengths are on the right. Previously used gases (like molecular nitrogen and argon) are noticeable. The He I 58.433 nm line is the brightest line and shows some saturation since this emission is very easy to excite to excite with the hollow cathode lamp. The color scale is greatly enhanced to highlight the dimmer features. The spray of green in the vicinity of 58.433 is extremely small scattered light and is within acceptable limits. Note that none of the lines are expected to be close to saturation when making measurements in flight.

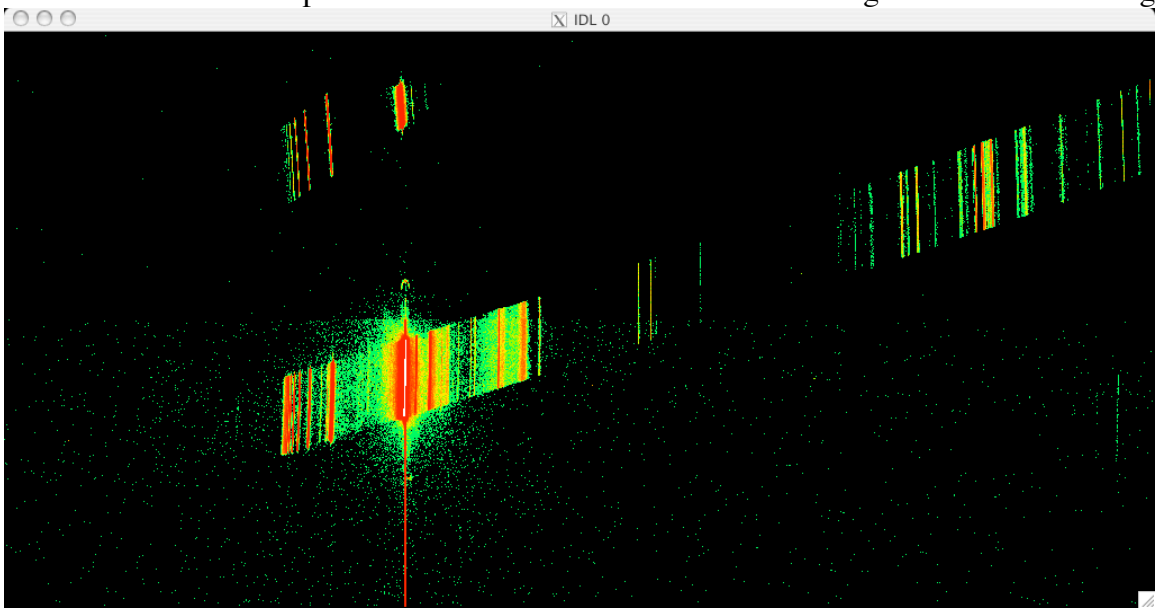

Figure 8. MEGS-B Helium raw signal (dark subtracted).

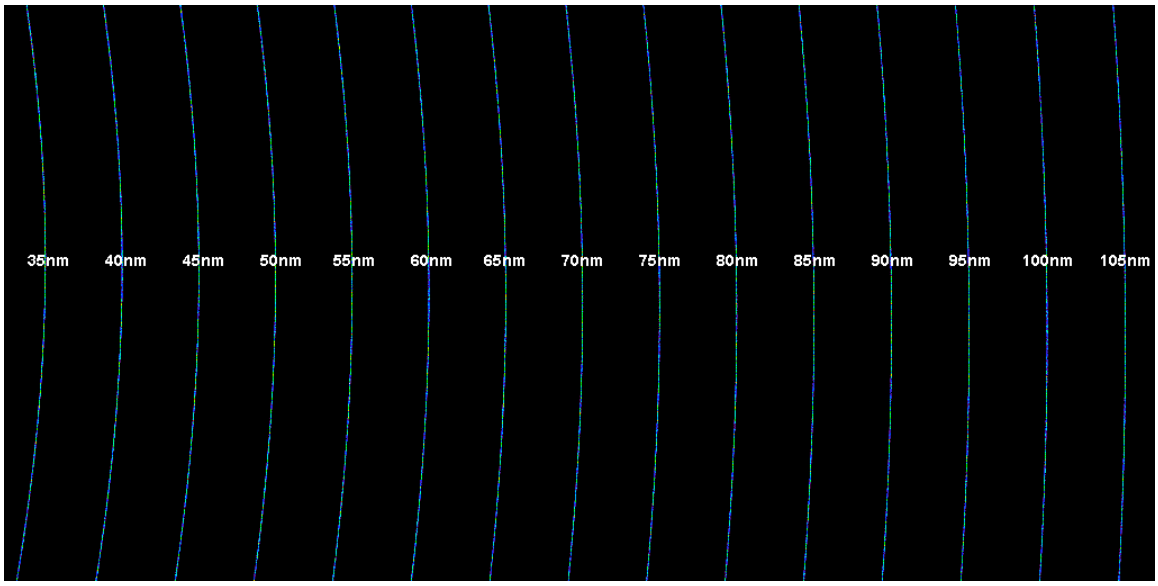

Figure 9. Ray-trace result for nominal pointing wavelength scale (first order only with baffles removed).

The lack of Helium lines in the wavelength region highlights the sensitivity of the detector to trace amounts from other species. Some of these are identified in Figure 10.

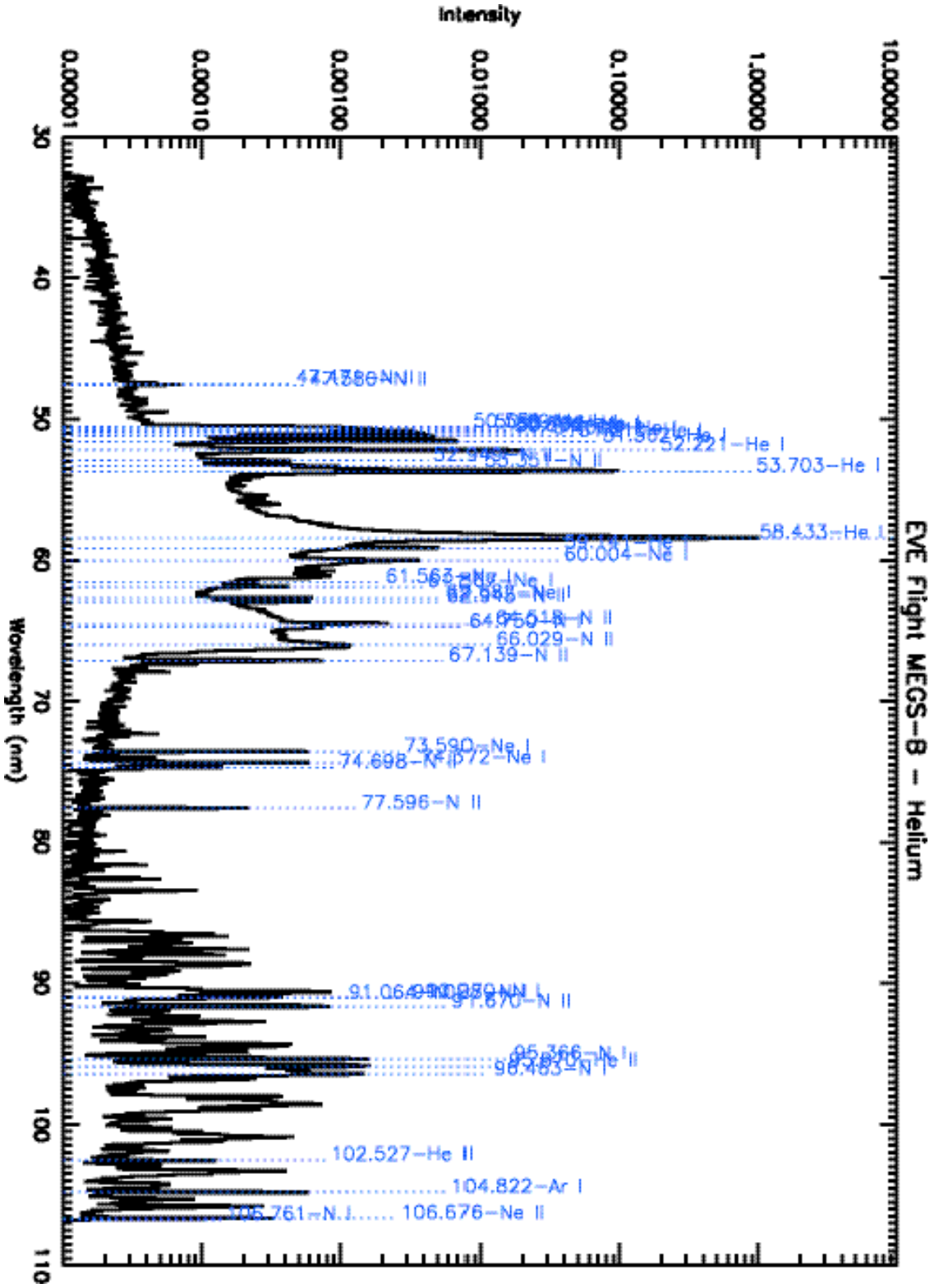

Figure 10. MEGS-B Helium spectrum with other trace gases.

3.2 Argon

Argon is better suited for determining the wavelength scale of MEGS-B due to greater spectral range as shown in Figure 11. Argon is a better candidate for determining resolution (FWHM method) because of the many isolated lines. Line widths are typically around 0.08-0.1 nm.

It should be noted that the resolution can be affected by pointing offsets. During the MOBI alignment on 06/09/07, a small offset is detectable which affects the position of the lines on the detector. The wavelengths used here were not fitted for this pointing angle and suffer some small loss of resolution because of it. 66 dim lines are within the 0.1 nm requirement, while the brightest line at 104.822 has a FWHM of 0.109 nm. Additionally, the hollow cathode lamp does not match the solar diameter, so the effects of off-pointing on resolution are enhanced in these ground measurements.

Note that previous measurements (with greater care taken to guarantee centering along SAM) produced these resolution estimates for several argon lines. This is the performance we expect on-orbit.

Wavelength (nm) & FWHM		Wavelength (nm) & FWHM	
55.658251	0.097537665	57.297854	0.091328866
57.924191	0.092858105	59.767393	0.093455573
60.285282	0.095180535	61.240032	0.094017194
67.840119	0.093713686	71.819051	0.089228604
73.100798	0.086553623	74.033498	0.090851922
80.991690	0.093759495	81.626242	0.093660844
82.009751	0.091883003	84.277510	0.086706488
89.421261	0.085975543	91.967253	0.084333471
93.194597	0.081992647	102.57831	0.085191478 (not argon)
104.84244	0.094516044		

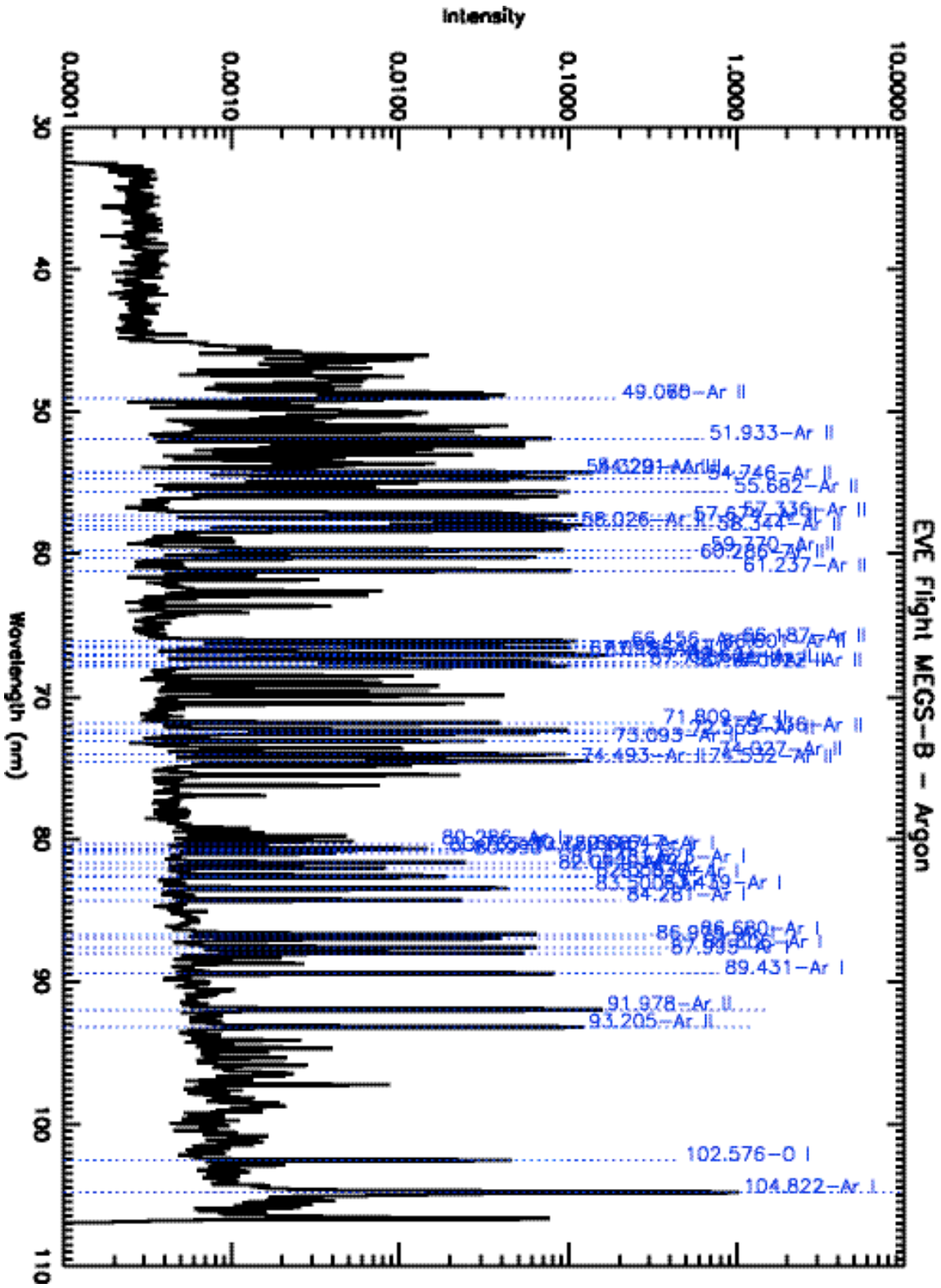

Figure 11. MEGS-B Argon spectrum.

3.3 Nitrogen

Molecular nitrogen has also been measured with MEGS-B and is shown in Figure 12.

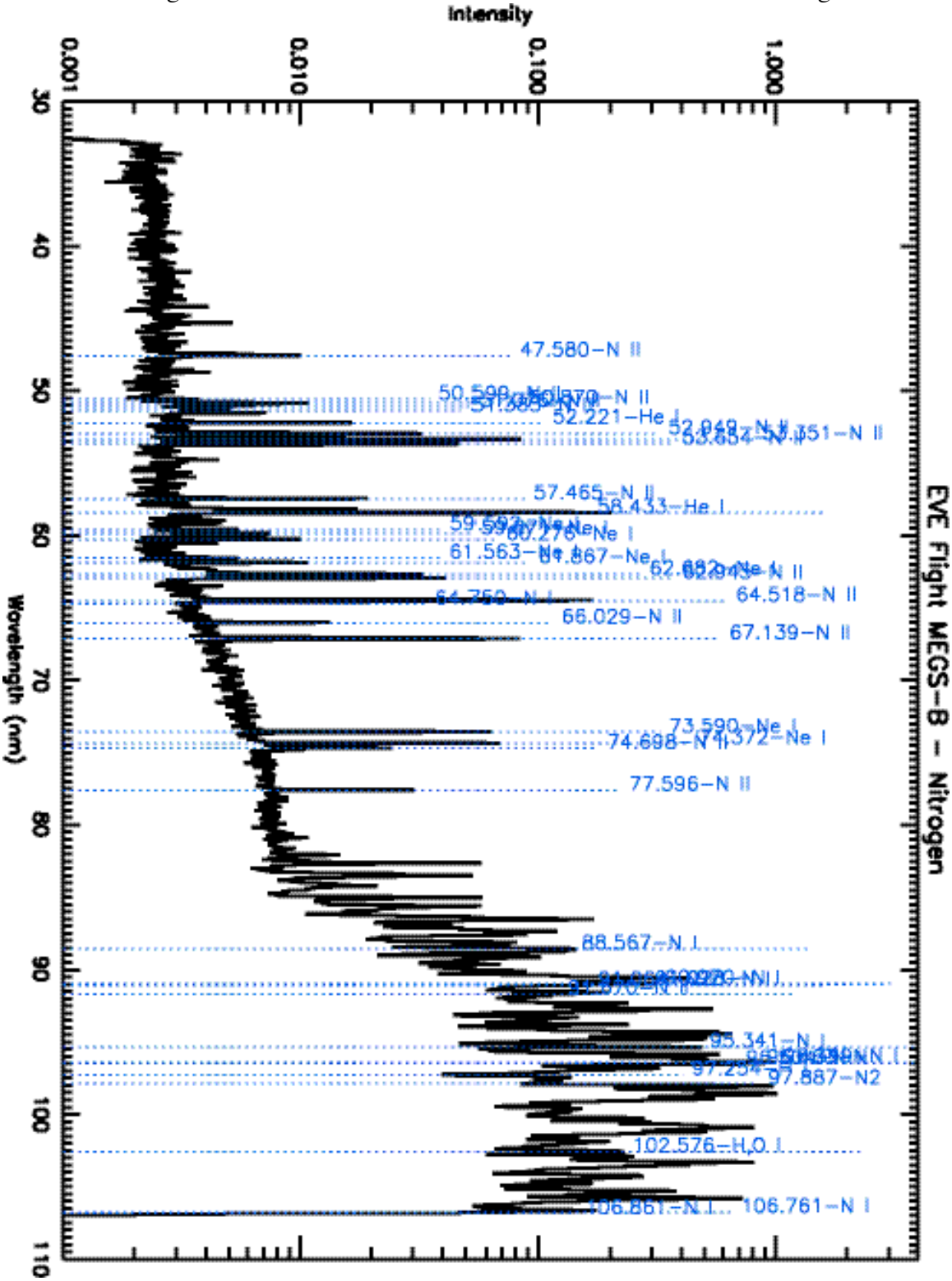

Figure 12. MEGS-B Molecular nitrogen spectrum.

3.4 Neon

MEGS-B has also been used to measure Neon as shown in Figure 13.

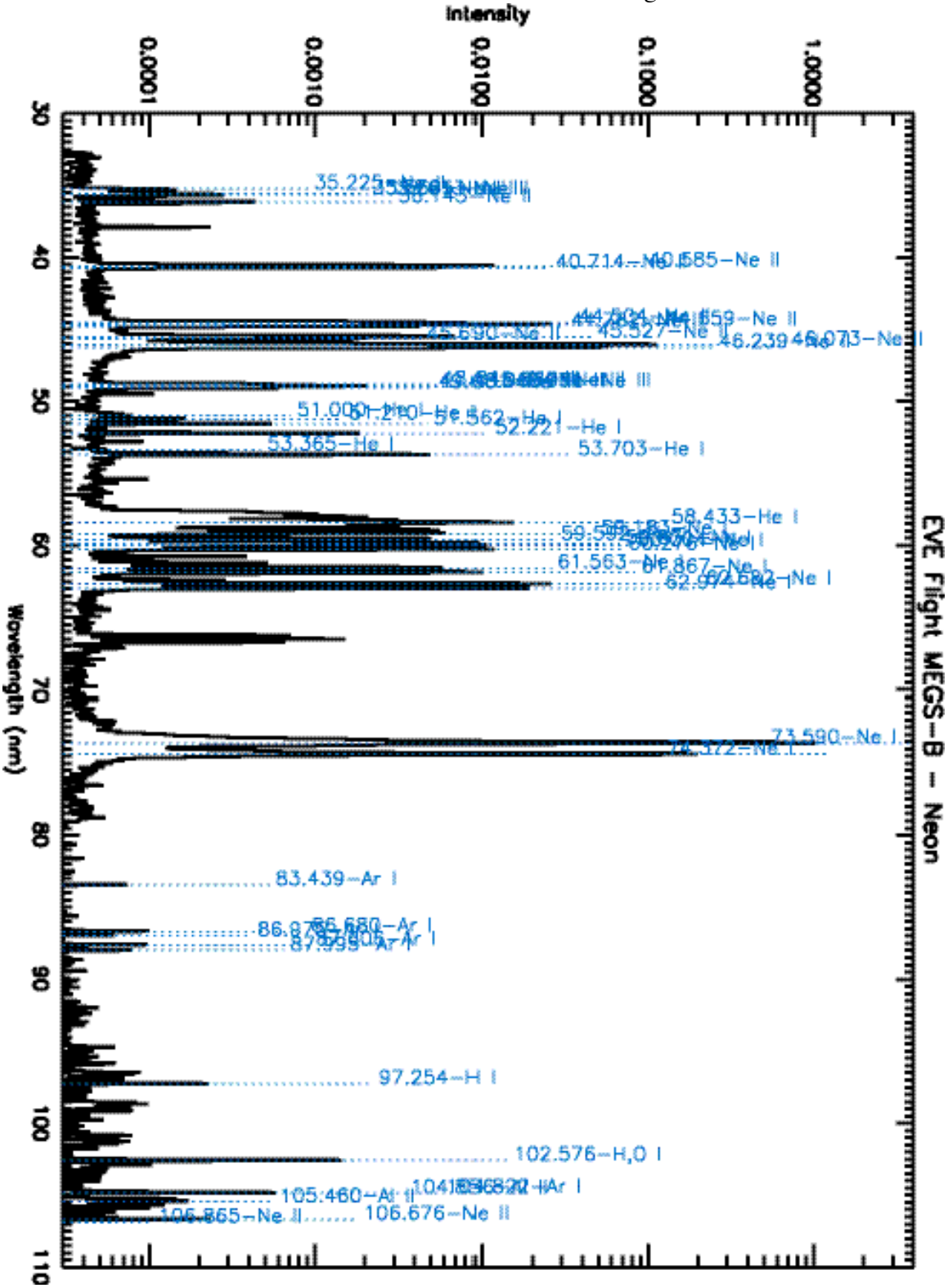

Figure 13. MEGS-B neon spectrum with several other species.

The wavelength scale is not optimal for the off-center pointing data shown in Figure 13, which lead to a misidentification to the shortest lines. This is only noted so that future wavelength scale adjustments can extend the best fits. The ideal situation would use the sum of neon and argon spectra to determine the wavelength scale. Unfortunately, difference in the source gas distribution in the HC may prevent this since each gas may require it's own centering (which may not have been performed).

4. MEGS-A and MEGS-B Overlap Comparison

Neon spectra were collected for MEGS-A and MEGS-B which has lines that lie in the overlap region. MEGS-A is sampled in Figure 14 at 0.01 nm bins although the resolution is about 0.07 nm. MEGS-B is sampled in Figure 15 at 0.025 nm bins although the resolution is about 0.1 nm. The comparison plots show the differences in spectral resolution.

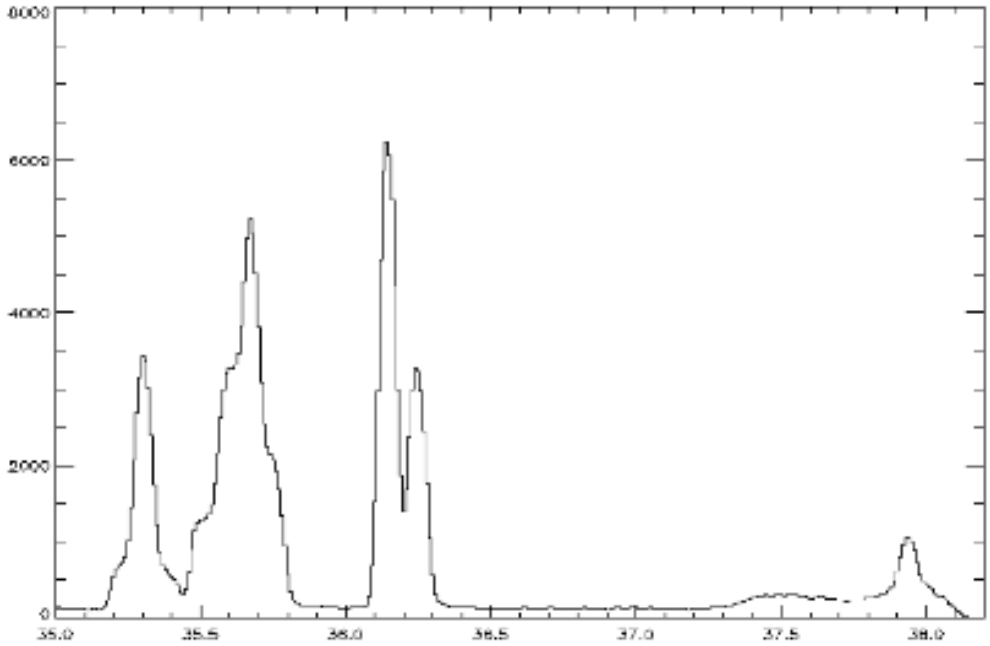

Figure 14. MEGS-A Neon spectrum in the overlap region.

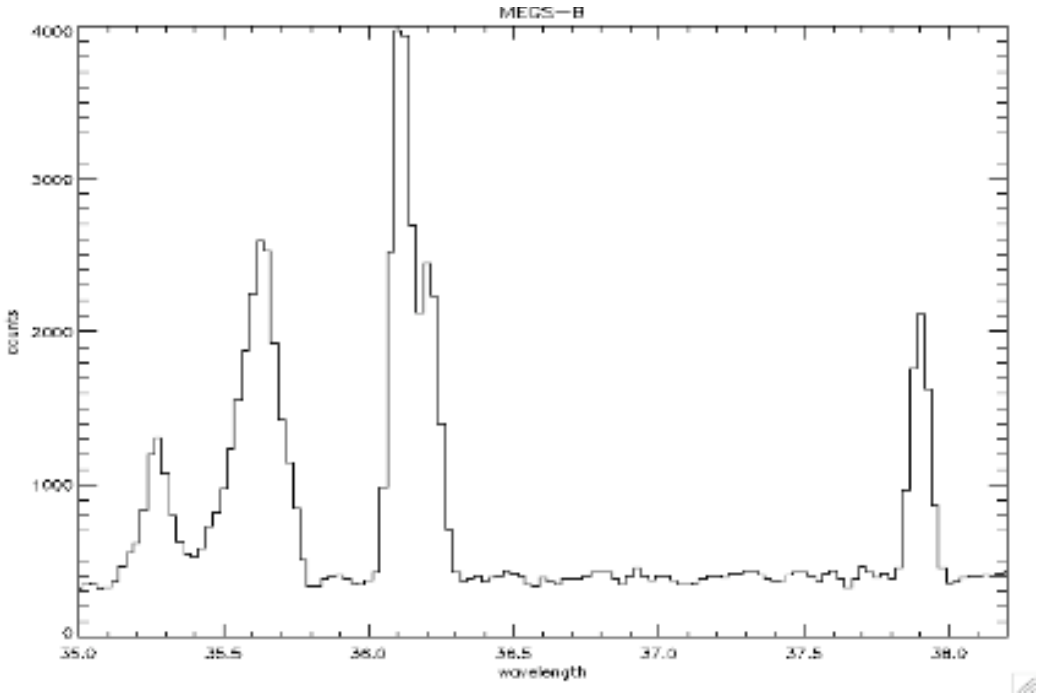

Figure 15. MEGS-B Neon spectrum in the overlap region.

All of the lines are Neon emissions in Figure 16. The black vertical dashes are the following lines Ne II 35.296, Ne II 36.143, Ne II 36.246, and Ne III 37.9306. Additional Ne II lines are closely spaced around Ne II 35.6800 represented by the dotted vertical lines. Differences in sensitivity at the extremes of the detector wavelength ranges have not been corrected. There may also be slightly different hollow cathode parameters. The figure is only intended to show that both CCDs overlap in wavelength by a few nanometers. The optimal wavelength scale for MEGS-B was not used which results in a small loss of resolution which can be seen in the shallow valley between 36.14 and 36.25 nm lines. A correction of 0.03 nm was applied.

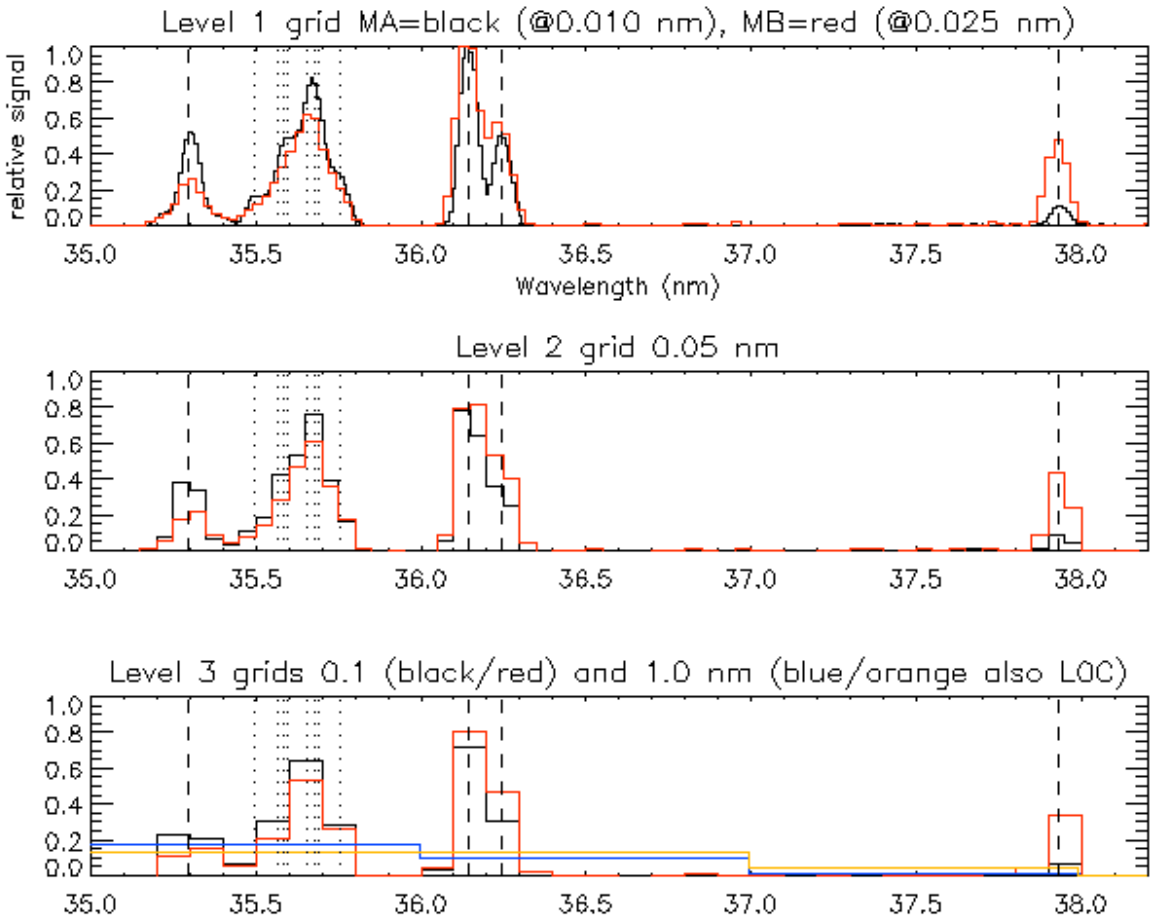

Figure 16. MEGS-A and MEGS-B Neon emission (relative signals) in the wavelength overlap region at all planned grids for the routine data processing levels.

5. Off-pointing Effects on Spectral Performance

Ground wavelength measurements were made where the instrument was translated horizontally on the MEGS translation stage (MTS) in the vacuum tank, and the hollow cathode lamp was translated vertically. The source gas was Helium in this case. These two stages were used to perform a crude cruciform scan to measure the spectral effects.

5.1 MEGS-A

For MEGS-A, 3 lines were tracked through the cruciform. The X (dispersion) and Y (cross-dispersion) center of mass coordinates of the lines as a function of lamp angle is shown in Figure 17 and Figure 18 respectively. There is approximately 1 pixel of movement over +/- 0.5 degrees in the X component. Almost all of the motion is confined to the cross-dispersion direction (Y) which is several hundred pixels. This is similar to the planned flight scan along the solar north-south axis.

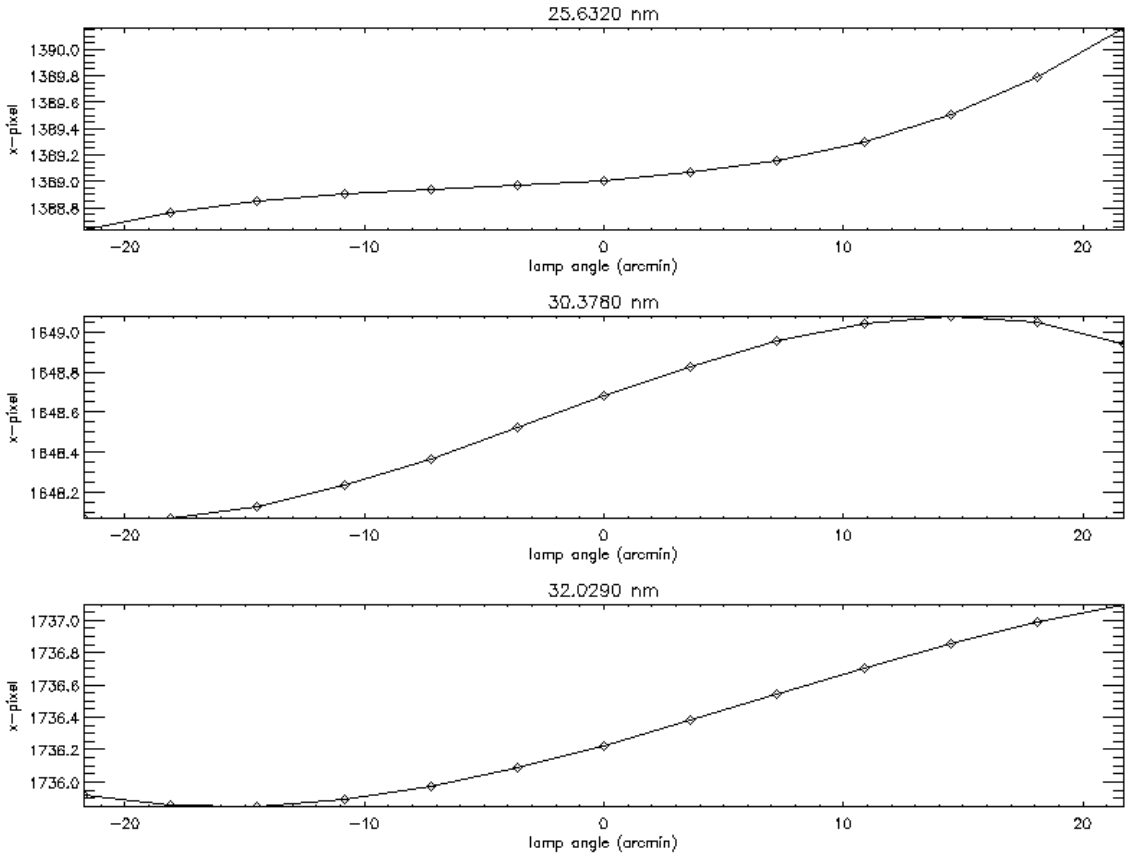

Figure 17. MEGS-A line-center motion vs. vertical lamp angle for the x-component (Y-scan).

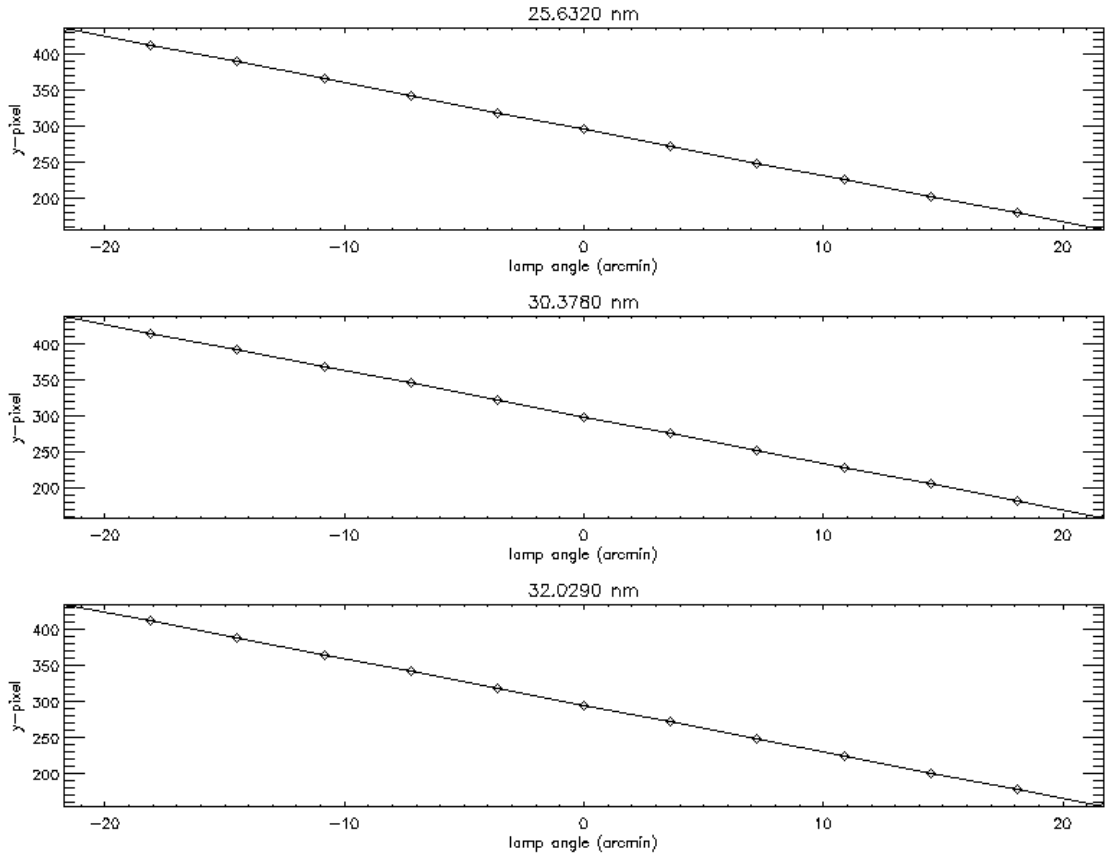

Figure 18. MEGS-A line-center motion vs. vertical lamp angle for the y-component (Y-scan).

The other scan (X) is similar to the solar East-West direction. This was performed by translating the MTS. The minimum in the X indicates that the best focus is achieved at the central pointing which verifies the alignment of the MEGS-A grating with the SAM science reference bore sight. Note also that MTS motion is coupled with Y motion since the line-centers move vertically. The MTS is not completely perpendicular to the lamp motion, but is within a few pixels at the 15-arcminute level.

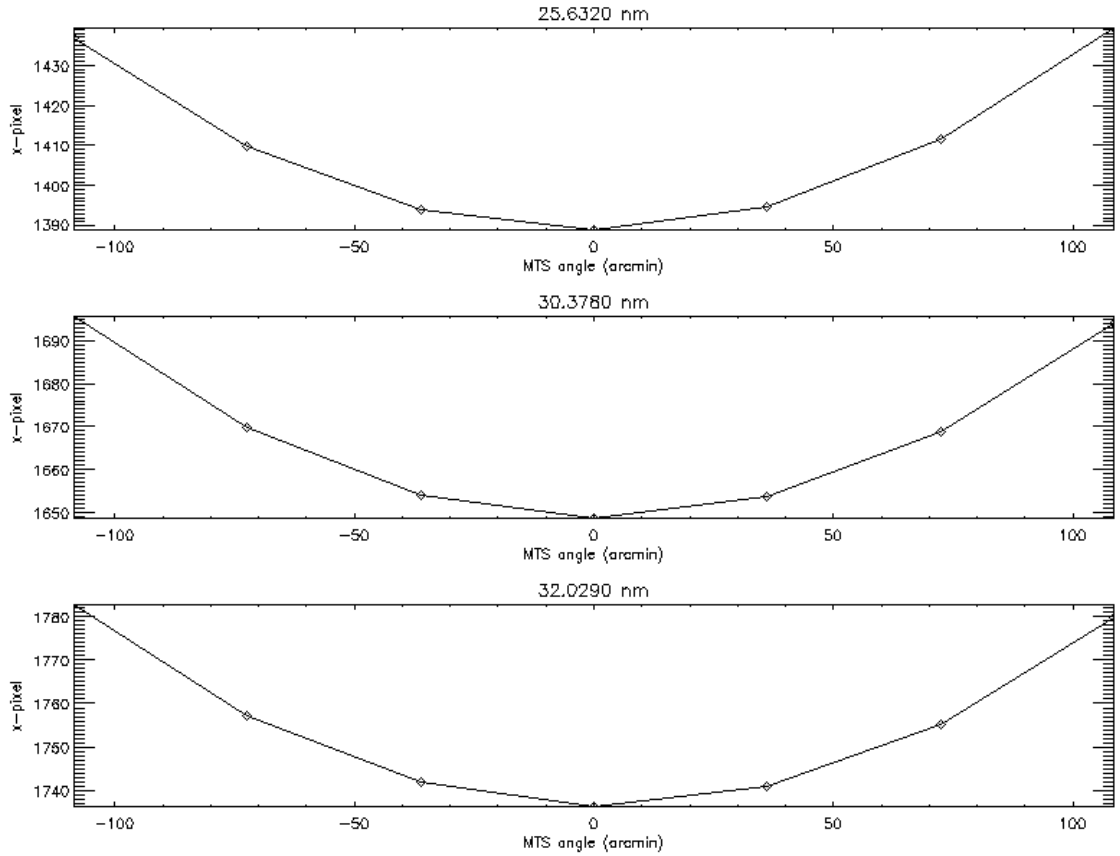

Figure 19. MEGS-A line center motion vs. horizontal MTS angle for the x-component (X scan).

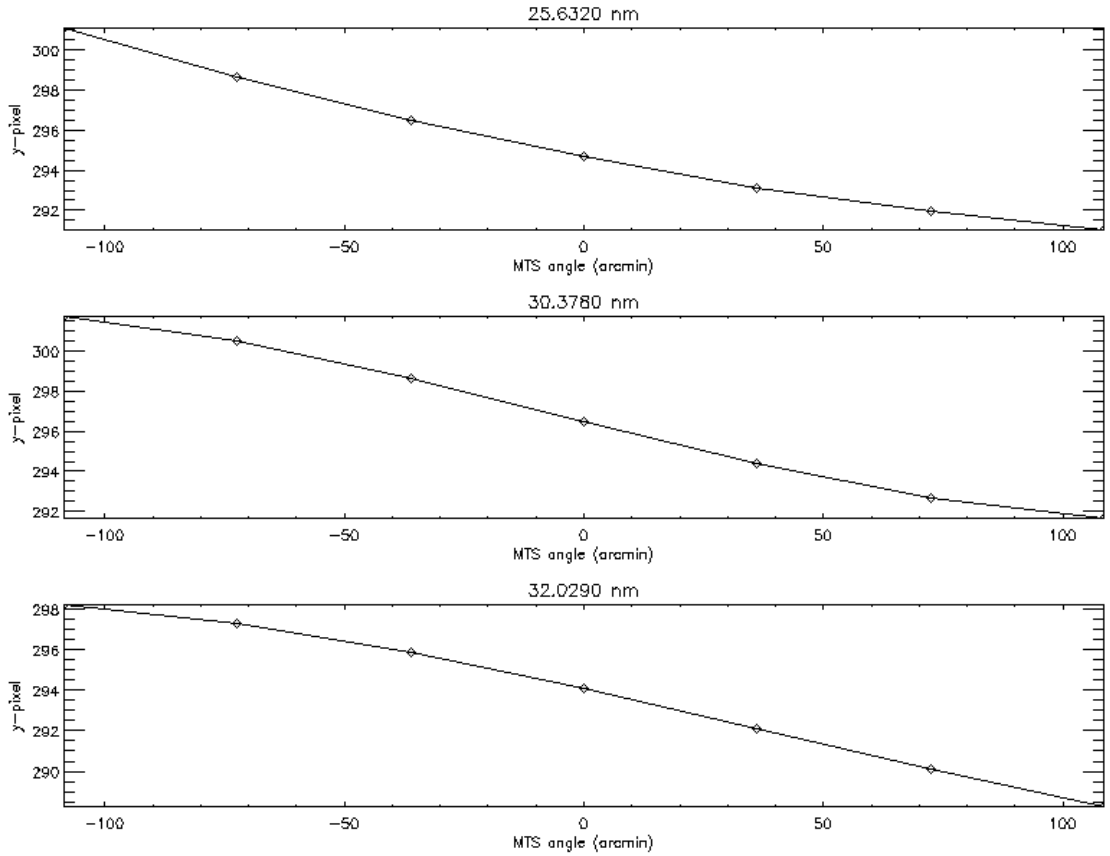

Figure 20. MEGS-A line center motion vs. horizontal MTS angle for the y-component (X scan).

5.2 MEGS-B

The motion of lines as a function of pointing angle for MEGS-B is significantly different than MEGS-A, and much less sensitive. All the data is plotted for both X and Y scans on each component plot, so the scale of the motion can be easily compared. Six different lines were tracked (Neon source gas) during the cruciform.

In the vertical scan moving the lamp (Y-scan), there is little movement in the x component. However, the movement is in opposite directions for short and long wavelengths. This can be pictured as an accordion-like spectral stretching.

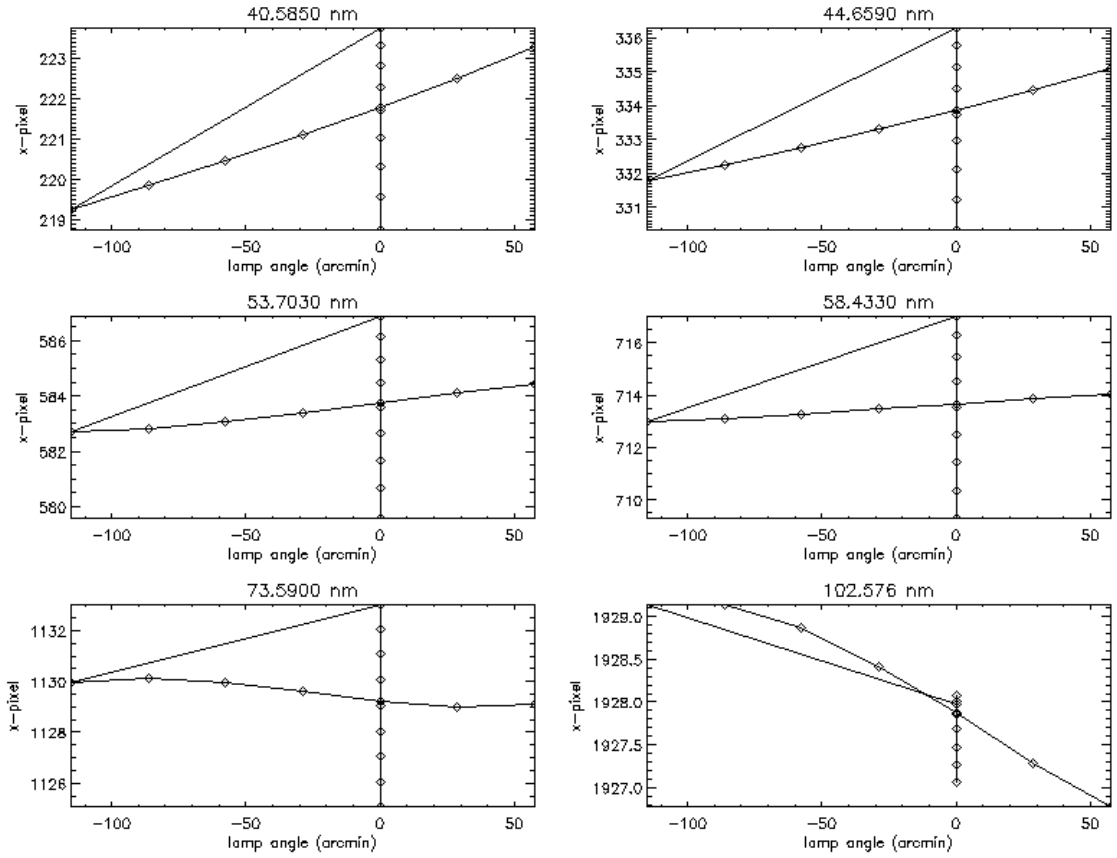

Figure 21. MEGS-B line center motion vs. vertical lamp angle for the x-component (Y scan).

More translation is observed in the line center Y-component. The motion is nearly linear with angle for all wavelengths except the longest one, which is curved.

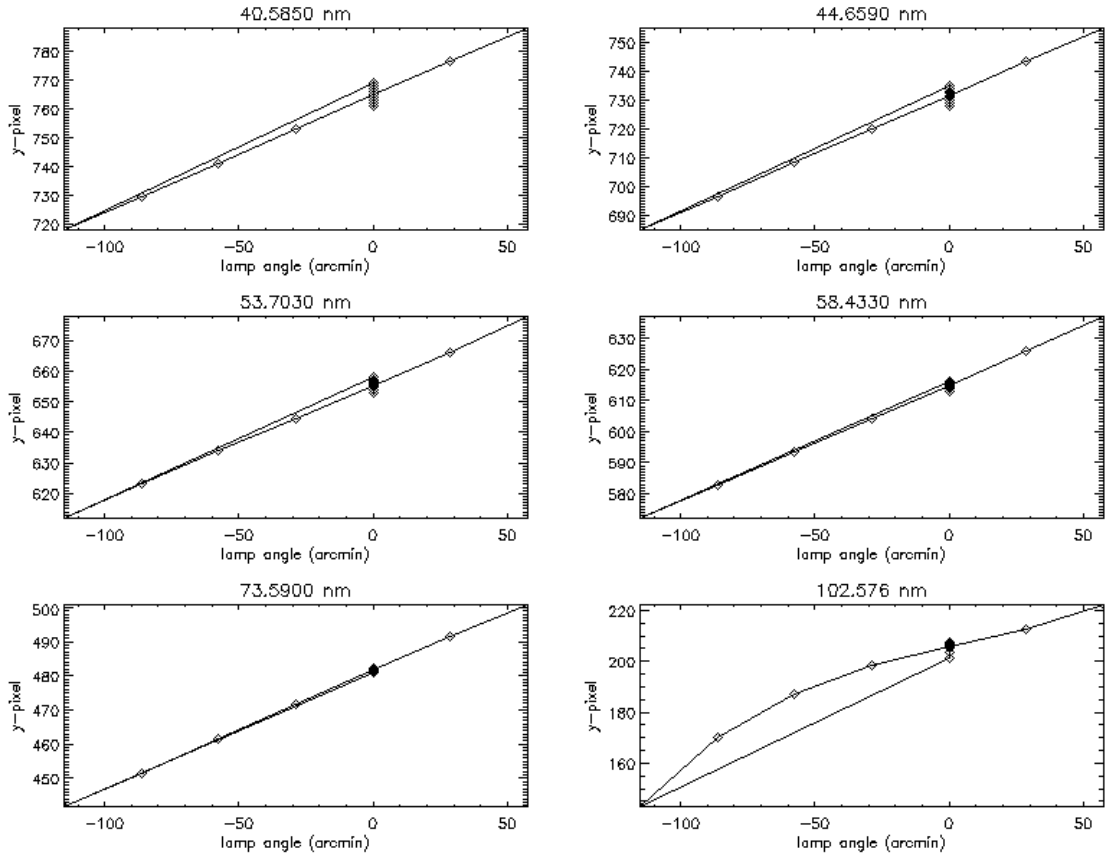

Figure 22. MEGS-B line center motion vs. vertical lamp angle for the y-component (Y scan).

For MTS movement (X-scan), there is little movement in the line center x-component. In fact, the amount is comparable to the lamp-scan motion for the short and long wavelengths, but greater for the middle wavelengths. MTS motion is not perfectly aligned with the optical axes, similar to what was found for MEGS-A.

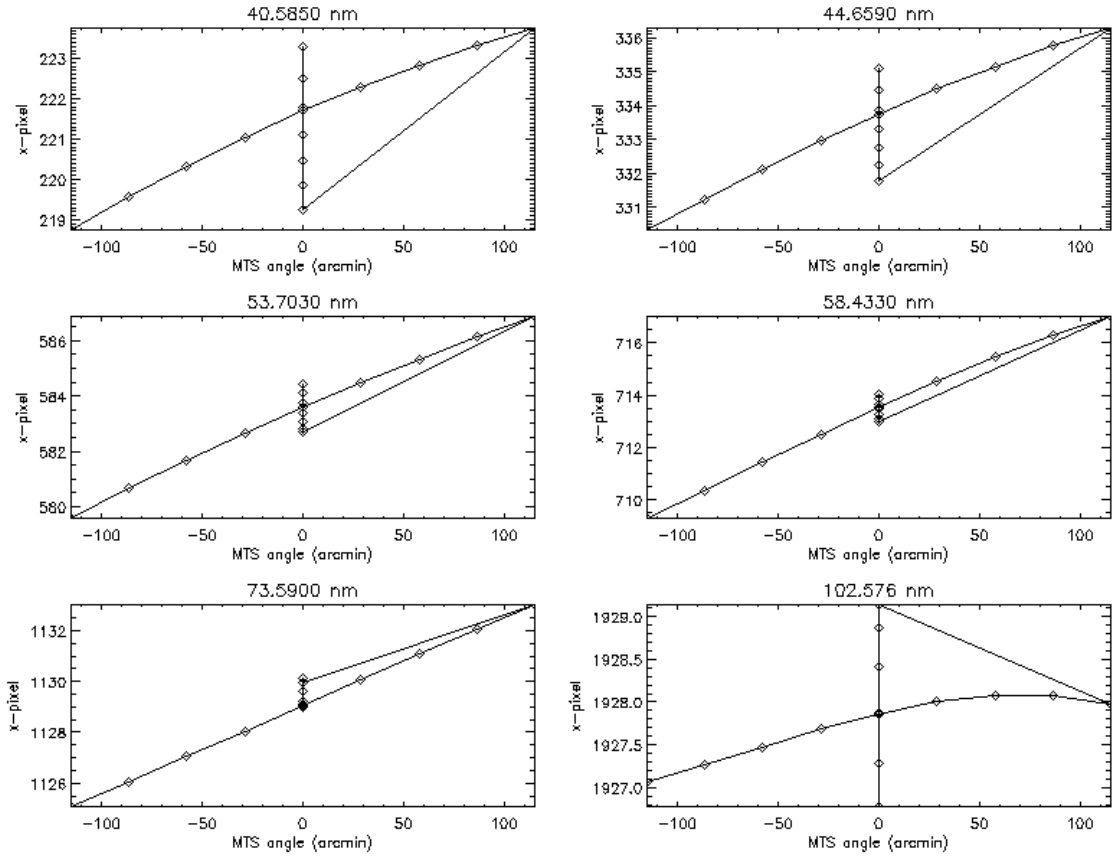

Figure 23. MEGS-B line center motion vs. vertical lamp angle for the x-component (X scan).

Almost no motion is noticeable for the Y-component of the MTS scan (X-scan).

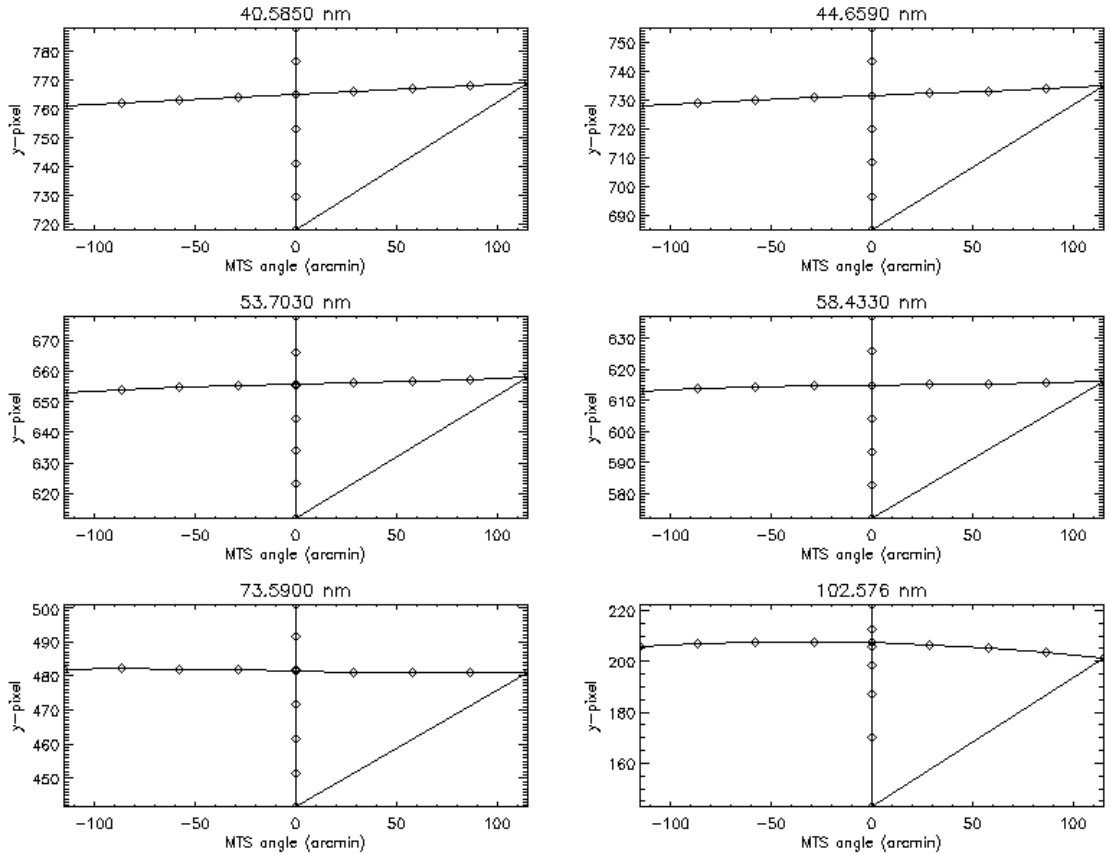

Figure 24. MEGS-B line center motion vs. vertical lamp angle for the y-component (X scan).

5.3 Instrument resolution changes

For a detailed discussion of changes in resolution, refer to the EVE Alignment and Focus Reports by Dave Crotser. These results have to be modeled since the true shape distribution of the solar disk radiation cannot be reproduced in the lab at this time. A summary of the ray-trace results is provided here in Figure 25 and Figure 26. For center pointing, excellent agreement is found with MOBI spectral measurements.

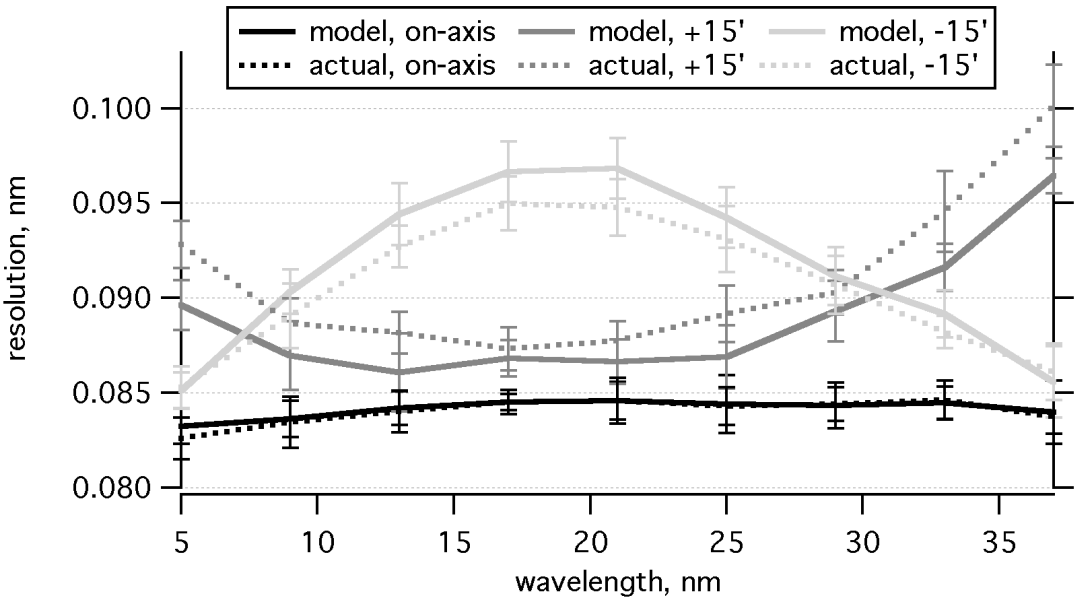

Figure 25. MEGS-A resolution vs. wavelength for multiple off-pointing angles.

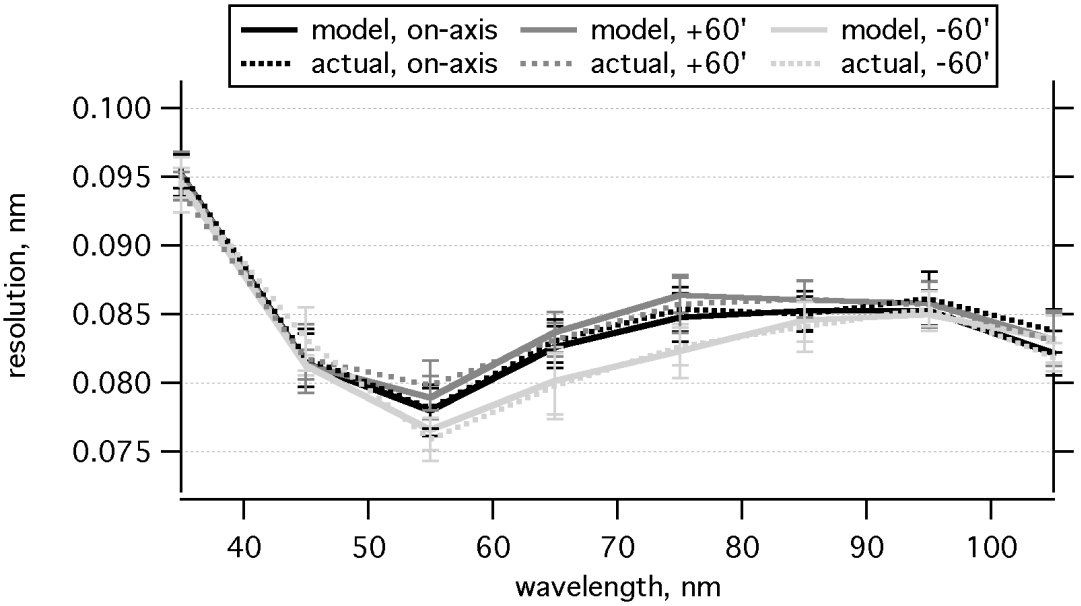

Figure 26. MEGS-B resolution vs. wavelength for multiple off-pointing angles.

6. Thermal Gradient Effects on Spectral Location

During instrument thermal/vacuum testing, the EVE instrument was driven warm and cold several times. During these warm-up transitions, several "stare" tests were performed to monitor the effects on the optical path. CCD temperatures ranges from -110 to -70 degrees C. Note this is in the vicinity of the operational temperature of -90 C. The EVE Electronics Box (EEB) was

driven from about -20 to +40, which is well beyond the planned operational range of 0-10 C. During the transition periods thermal gradients across the case caused very small deformations that were measurable by the CCDs.

6.1 MEGS-A

The MEGS-A component performed a stare at the Hollow Cathode lamp with Helium gas flowing. The motions of two lines were analyzed and are shown in Figure 27 and Figure 28. The main result is that over the operational temperature range, the lines do not move significantly.

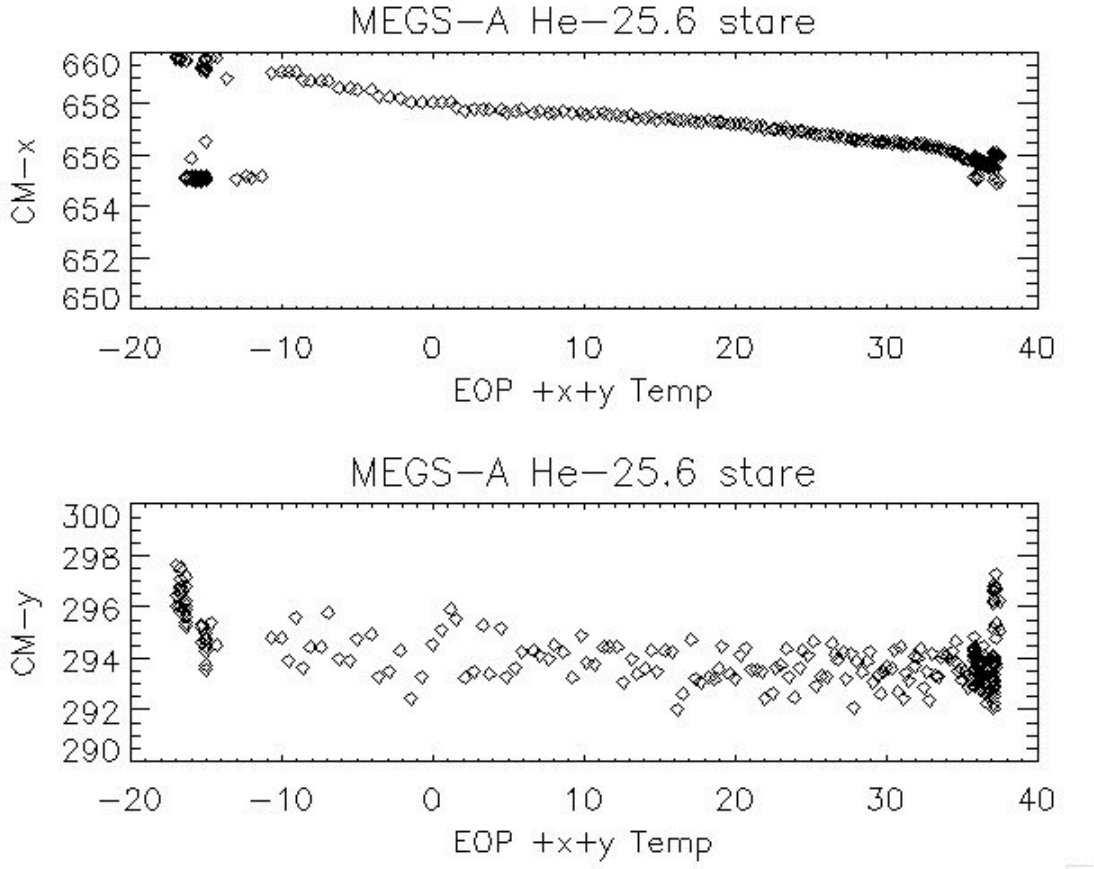

Figure 27. MEGS-A Thermal gradient stare test results.

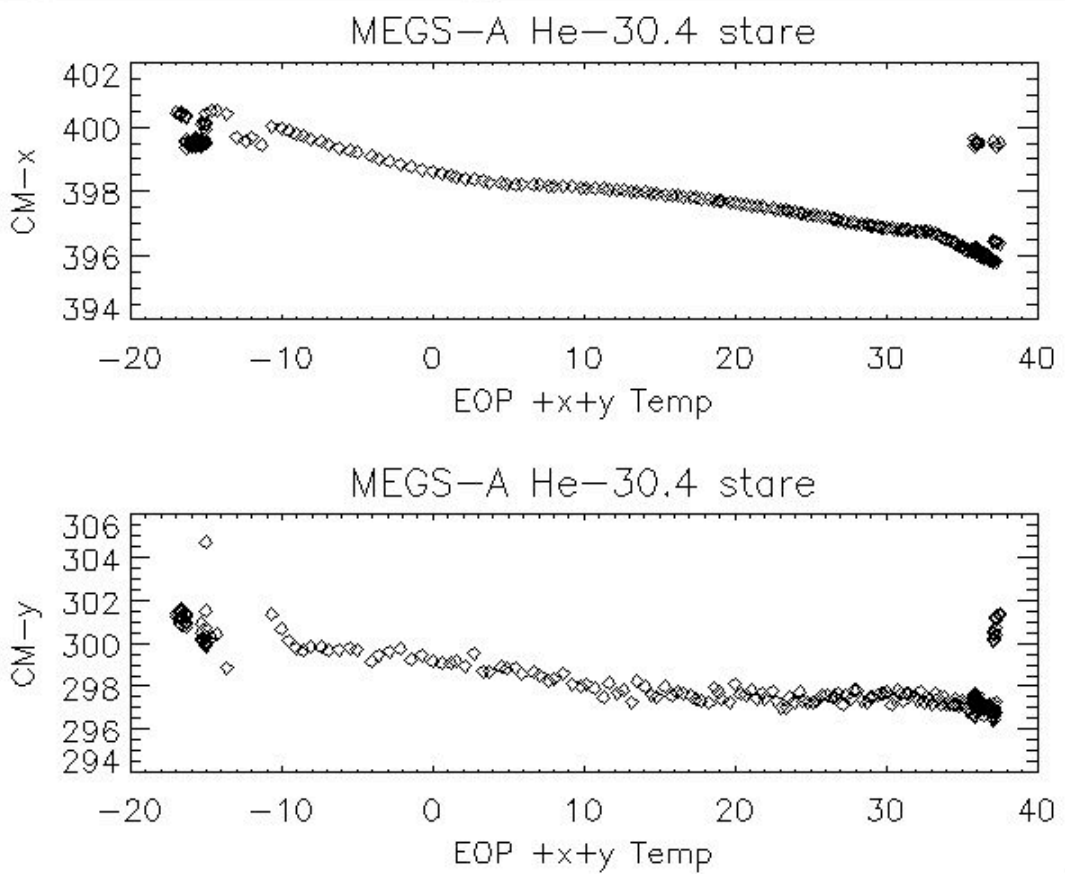

Figure 28. MEGS-A Thermal gradient stare test results.

6.2 MEGS-B

The MEGS-B component performed a stare at the Hollow Cathode lamp with Argon gas flowing. The motions of two lines were analyzed and are shown in Figure 29 and Figure 30. The main result is that over the operational temperature range, the lines do not move significantly. Outside the operational range, larger deviations are found. Those deviations are still within the useable range of MEGS-B.

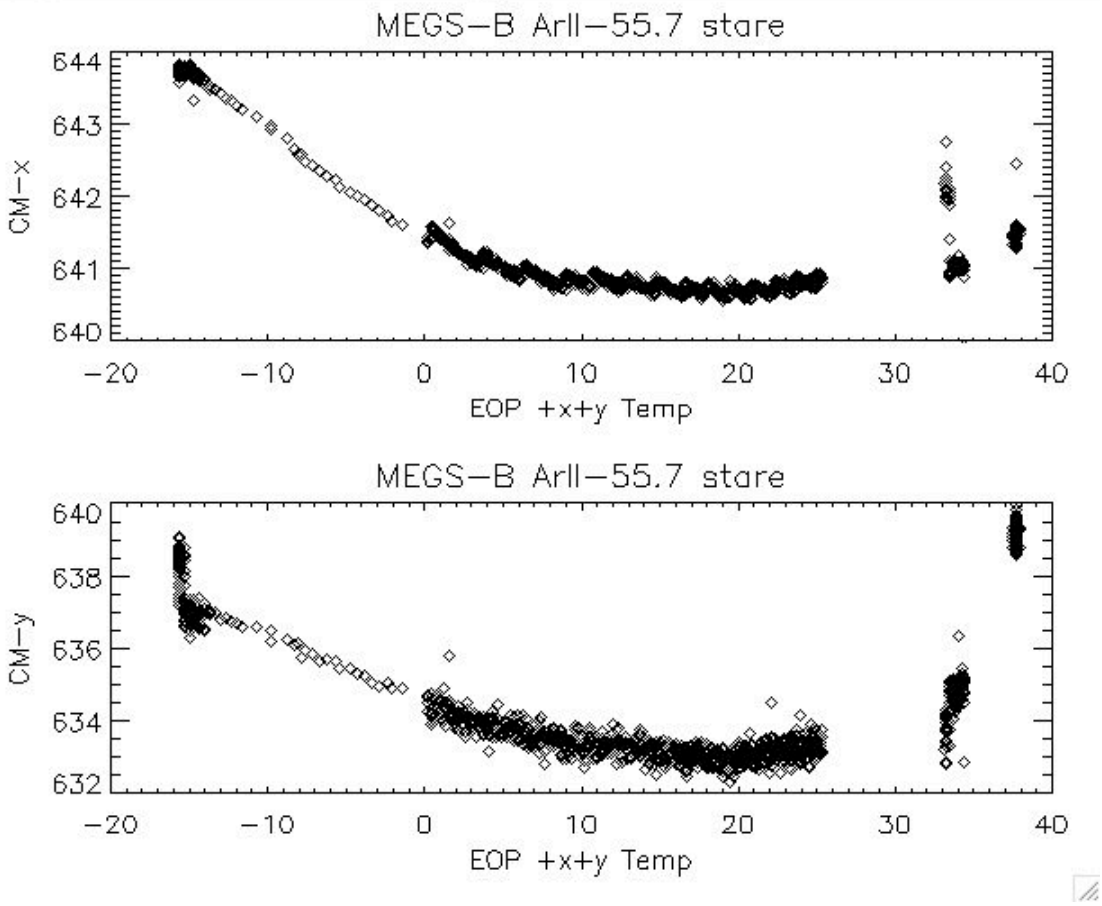

Figure 29. MEGS-B Thermal gradient stare test results.

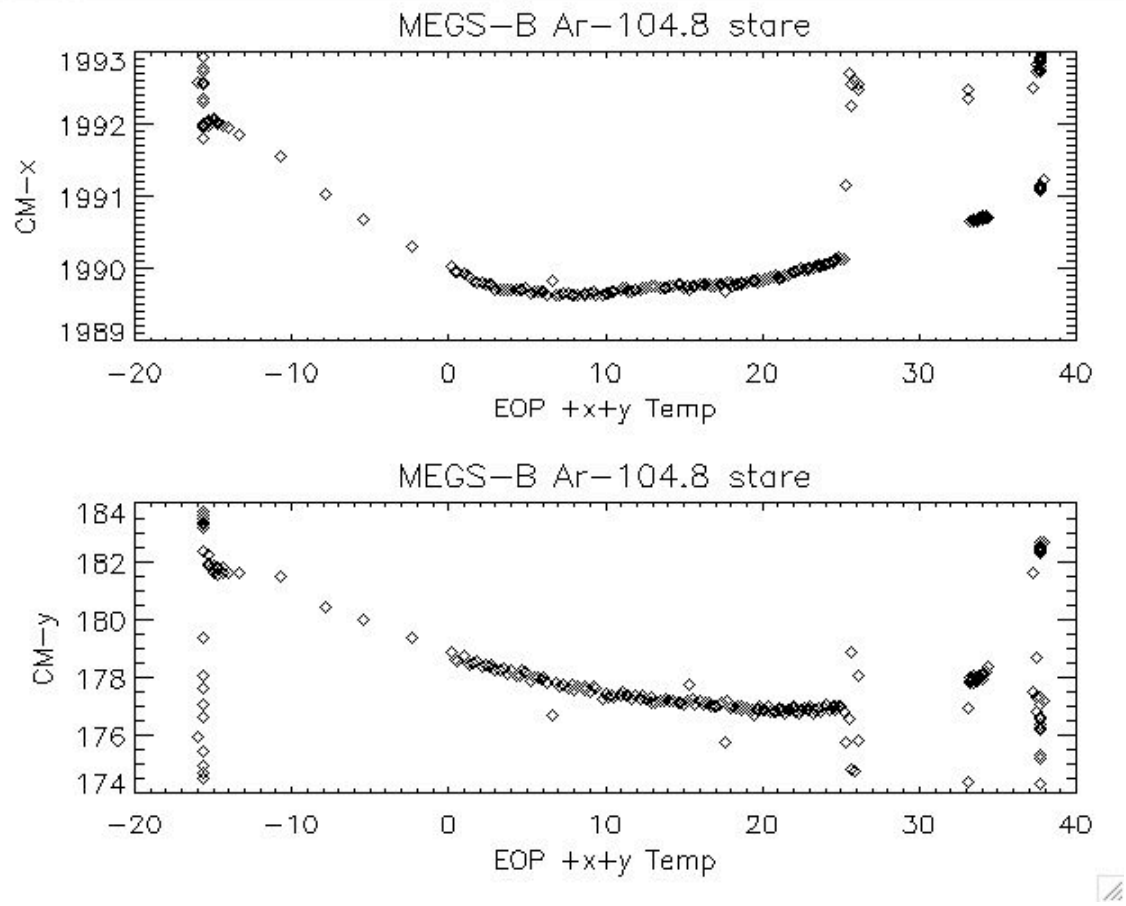

Figure 30. MEGS-B Thermal gradient stare test results.

7. Modeled Detector Performance

7.1 Detector Measurement

The next pair of images shows greatly contrast-enhanced images of the expected solar signals (without SAM, images generated by Dave Crotser) on top of measured background signals (MOBI).

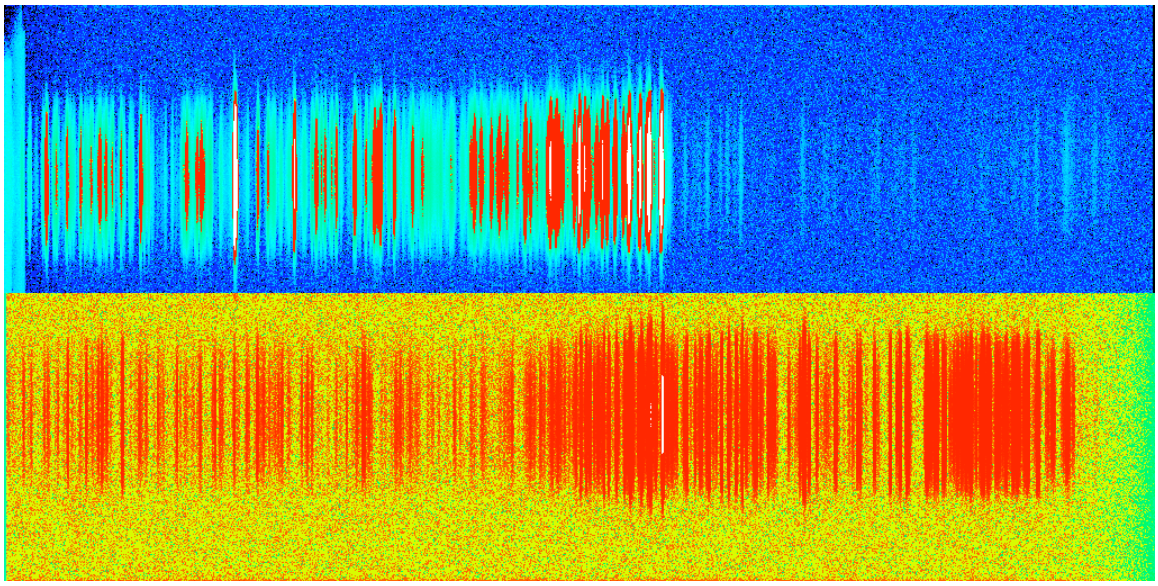

Figure 31. Expected MEGS-A solar spectrum (without SAM).

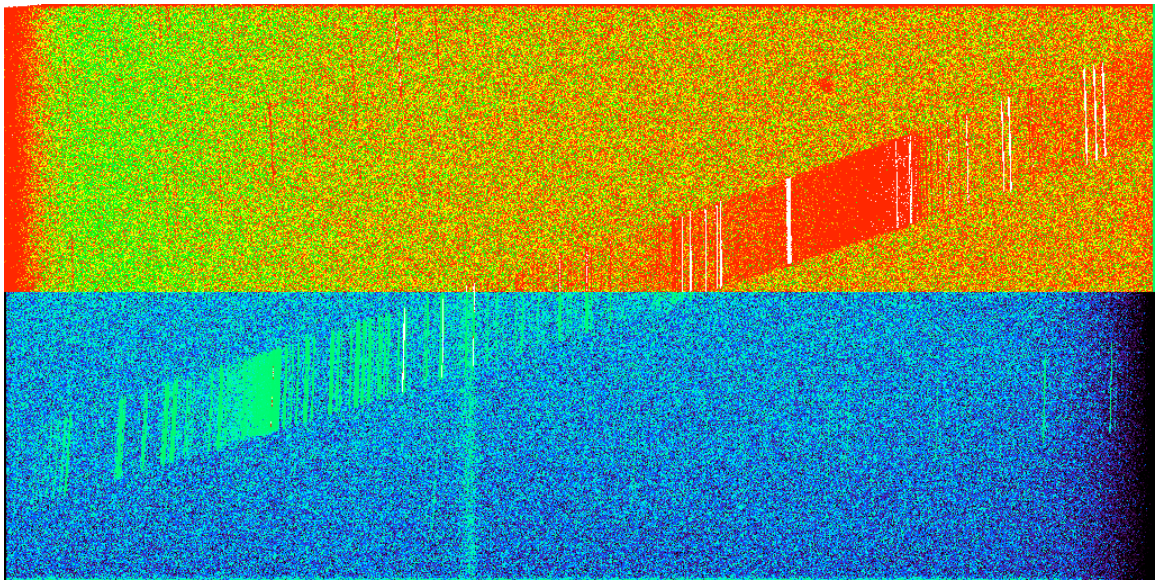

Figure 32. Expected MEGS-B solar spectrum.

7.2 Predicted Signal Levels

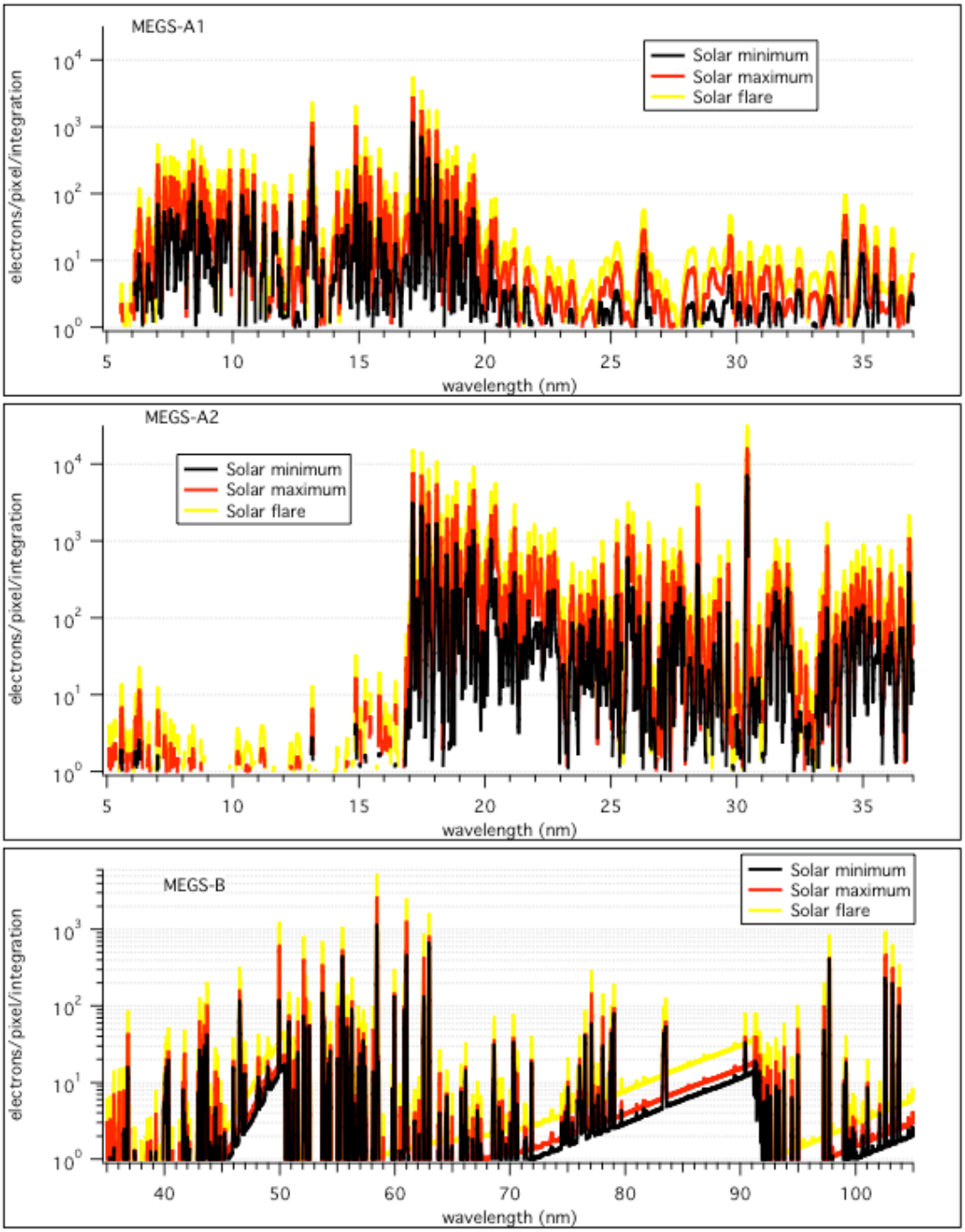

Figure 33. MEGS Predicted Signal Estimates (03/09/07).

7.3 Effect of Active Region Spatial Distributions on Spectra

Dave Crotser did a ray-trace study of the effect of a large flare on a solar line. In his study he shows that there is some spatial information available in the line profiles.

7.3.1 Solar Longitude Dependence

EIT 171Å Flare study: Solar max image compared to Solar max image with one active area's signal increased by factor of x10 (area ≈ 0.5% of disk):

171Å Solar Max

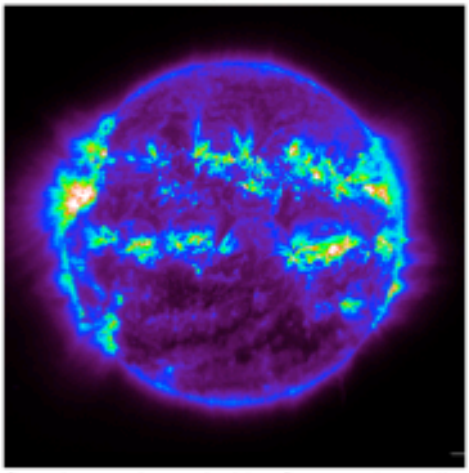

171 Å Solar Flare (bright region x10)*

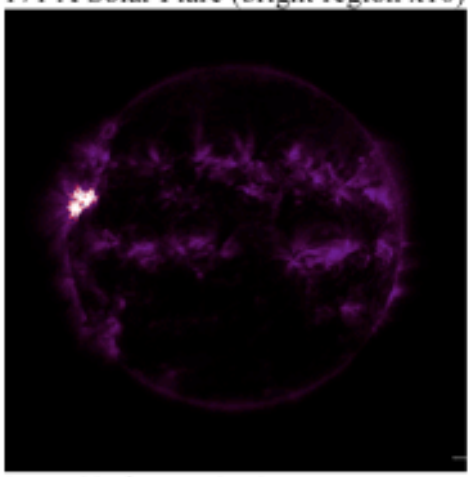

*Solar flare image is scaled by flare region; all pixels outside flare region have same count value for Solar max and Solar flare, which isn't evident from color scale

cross-dispersion direction line profile:

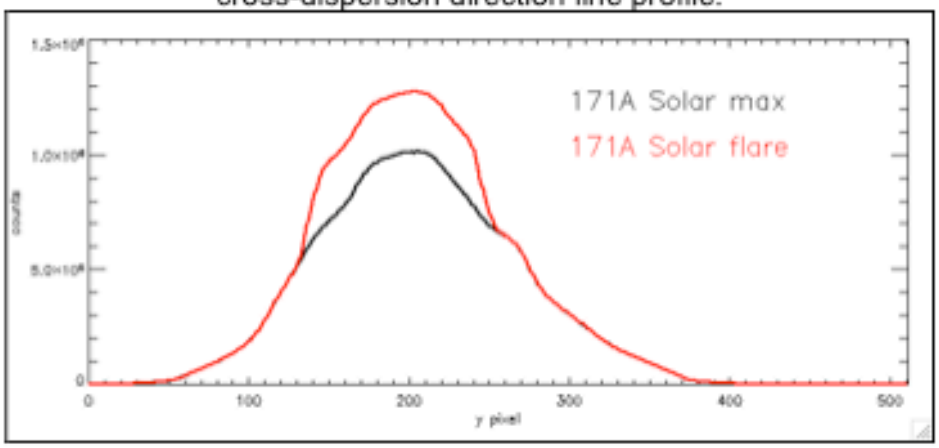

dispersion direction line profile:

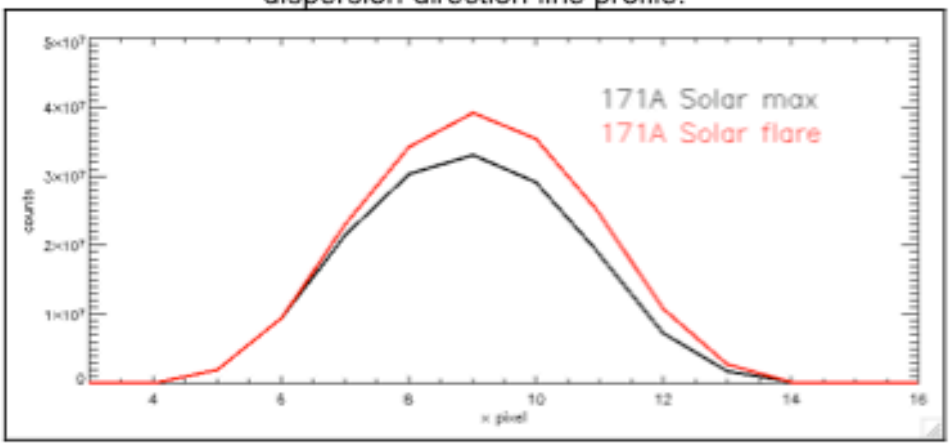

7.3.2 Solar Latitude Dependence

If the active region is rotated about the line of sight towards the sun (equivalent to a spacecraft roll), then the profile changes as shown in the following graph. These are similar steps to the HMI roll maneuver. Although there is spatial information in the line shape, it cannot be easily extracted.

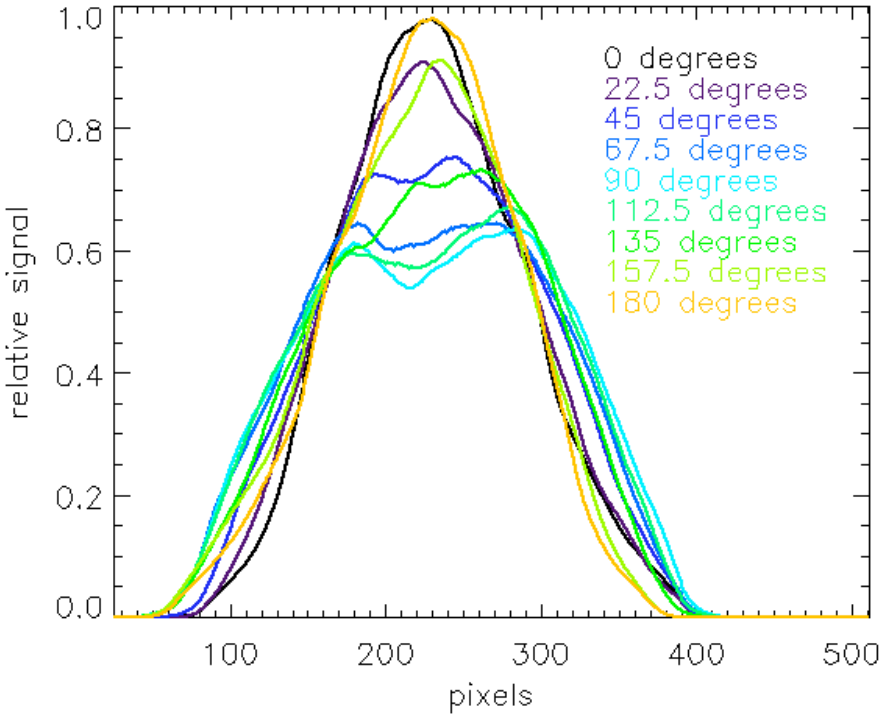

7.4 Percent of Signal Needed for Accurate Measurement

How much of the signal is required to obtain a given percent of the total signal?

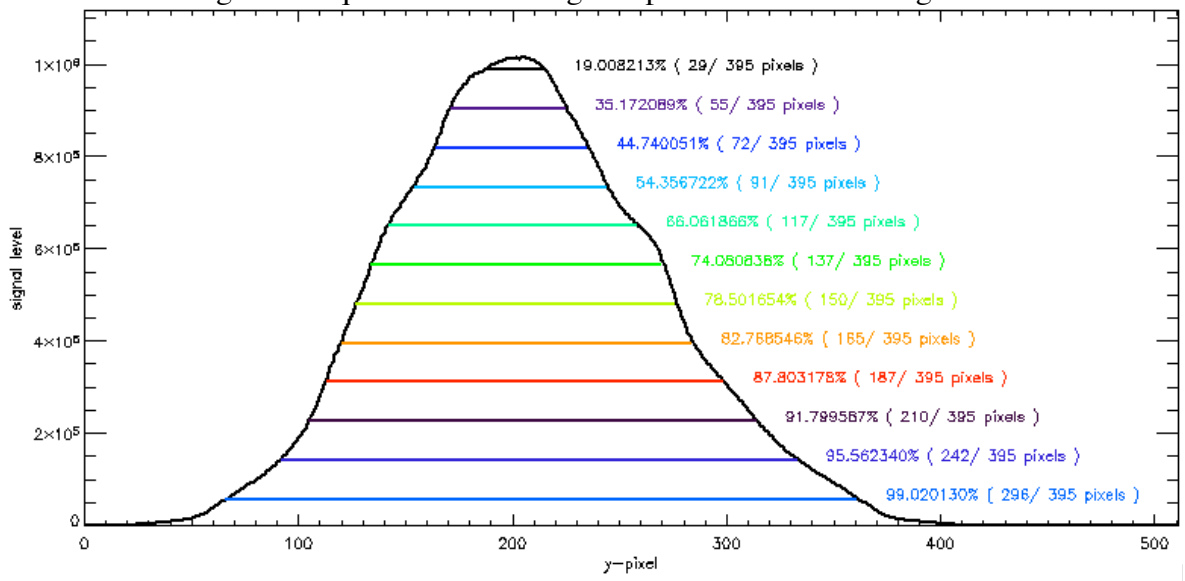

8. Scattered Light

Scattered light off the grating has been measured and the grating performance does not require a processing correction.

8.1 MEGS-A

8.1.1 Grating Scatter in the Cross-Dispersion Direction

8.1.2 Grating Scatter in the Dispersion Direction

8.2 MEGS-B

This section described an analysis of the grating scatter around the brightest line (just saturated) for Neon in MEGS-B. This line spans the top/bottom boundary and represents the "worst-case" situation.

8.2.1 Grating Scatter in the Cross-Dispersion Direction

Below are a few plots smoothed by 3 pixels. Each color is a consecutive column slice, stepping across the line. The line curvature makes the column look either concave or convex (except where it is saturated). The red/yellow columns show smearing from the bottom right tap.

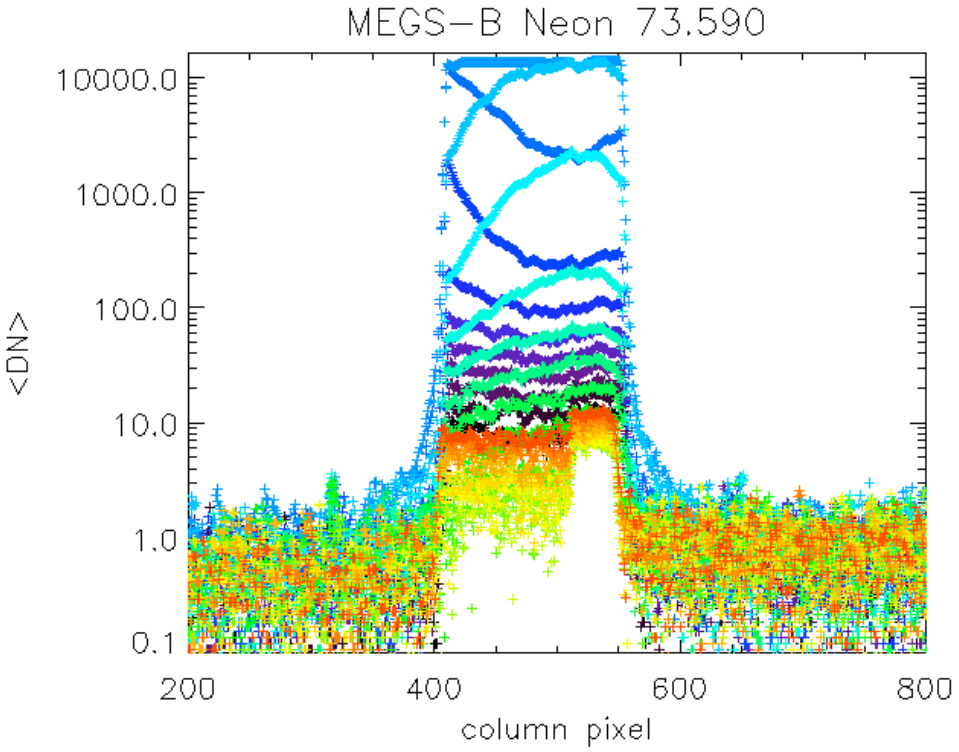

The next plot confirms the SURF results showing that the vertical scatter for this saturated line is negligible.

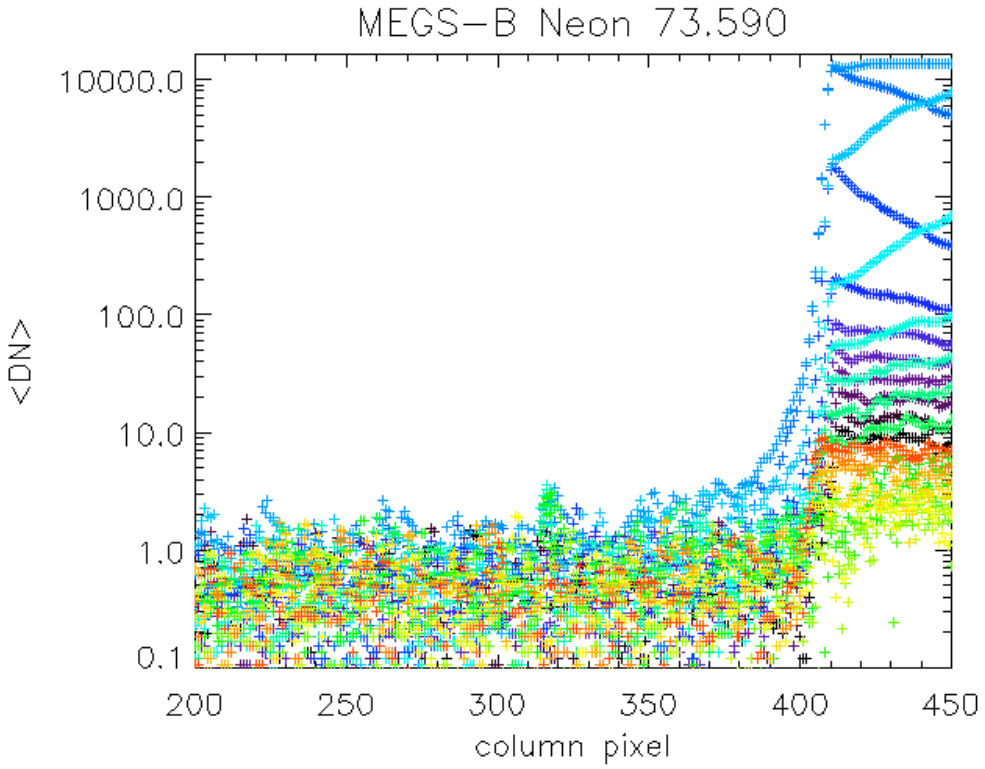

8.2.2 Grating Scatter in the Dispersion Direction

The next image is a series of row slices for the same Neon line and the next dimmer line at 74.372. The top/bottom parts represent top/bottom taps respectively (we can only look at the right side of the bottom due to smearing). On the top tap, the intensity drops to less than 1% at 4 pixels to the left of the peak, and 3 pixels to the right. The 1% value on the bottom tap is also between 3-4 pixels away from the peak despite the very long smearing wings. This indicates that scatter in the dispersion direction is also negligible (near the center) since it's comparable to the resolution of the measurement.

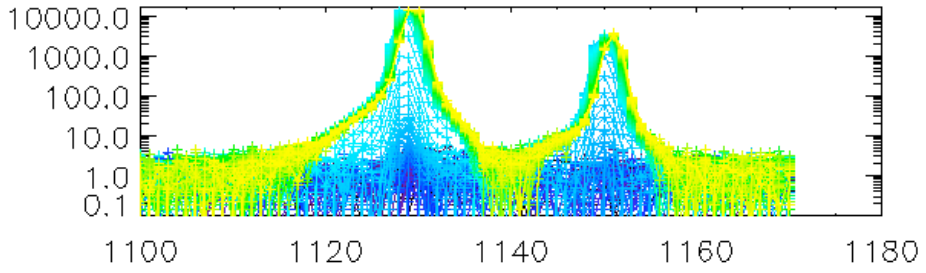

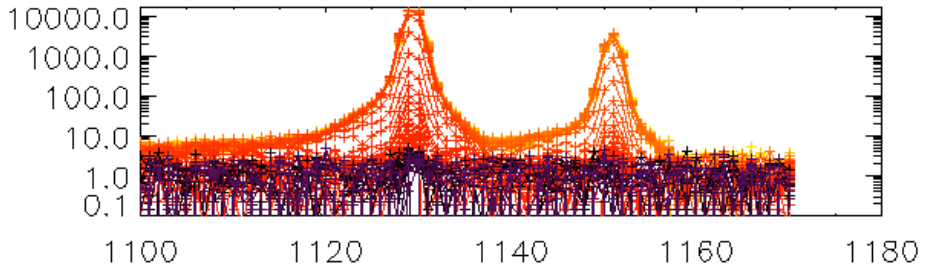

9. MEGS-A Diffraction Analysis/Removal

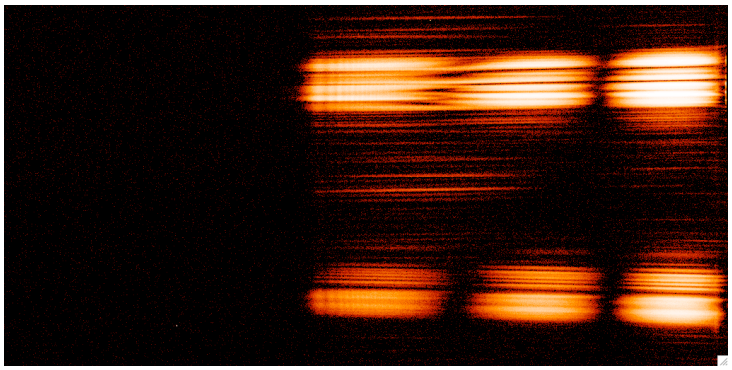

Figure 34. Red (632.816 nm) laser slit 2, position 5, 2007203-10:08:10, Mode 1 (TLBR).

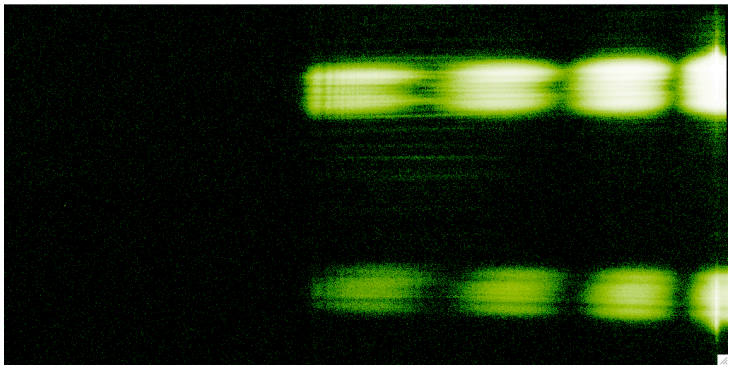

Figure 35. Green (543? nm) laser slit 2, position 5, 2007203-11:14:00, Mode 1 (TLBR).

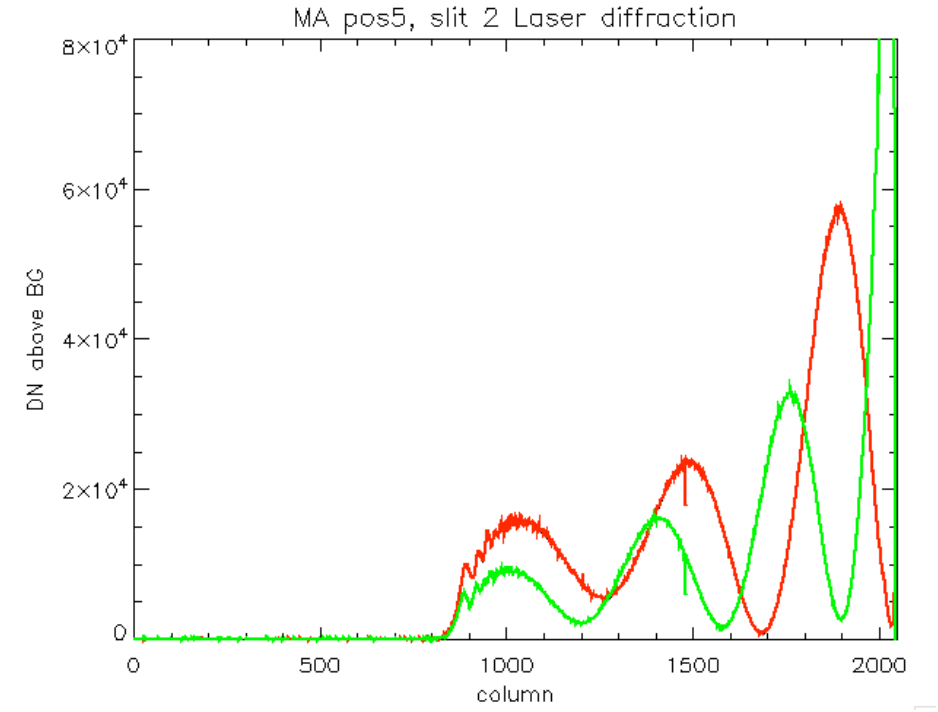
MA pos5, slit 2 Laser diffraction
8×10^4
6×10^4
4×10^4
2×10^4
0
DN above BG
0
500
1000
1500
2000
column

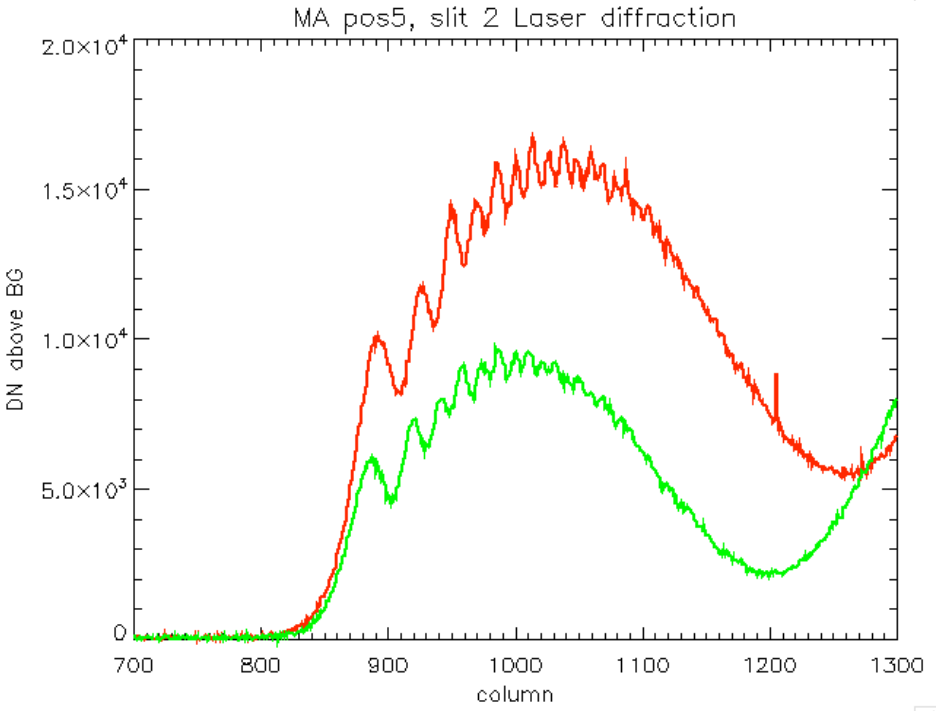
MA pos5, slit 2 Laser diffraction
2.0×10^4
1.5×10^4
1.0×10^4
5.0×10^3
0
DN above BG
700
800
900
1000
1100
1200
1300
column

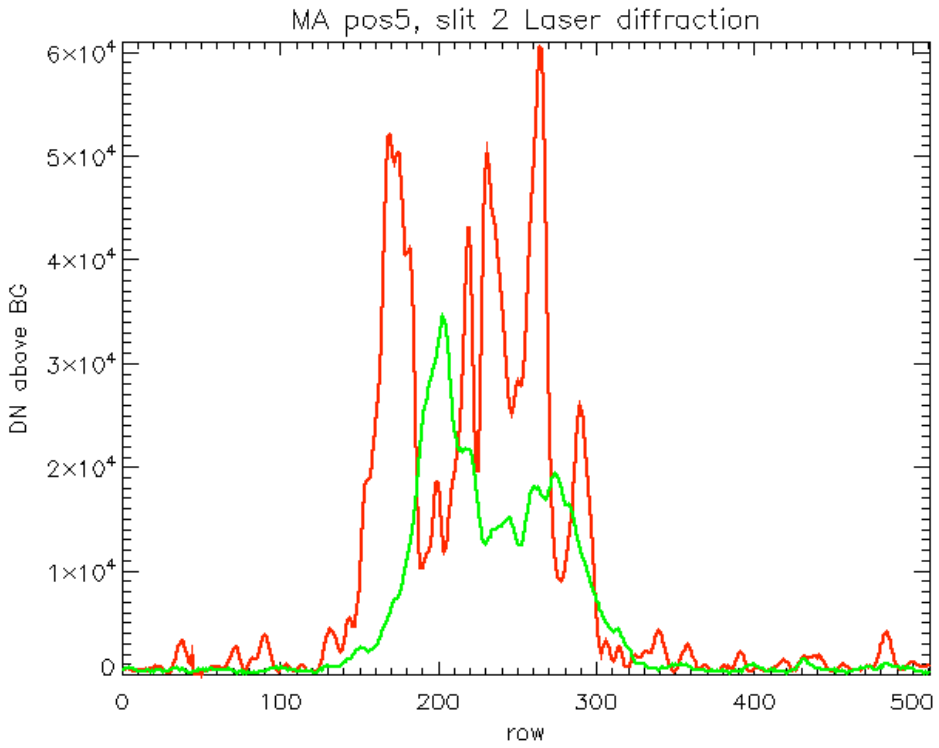

The next plot shows 4 curves all of which are the signals in the slit 2 columns. Black is the same stationary image shown first, red is the first image during movement, blue is the 2nd image during movement, orange/yellow is the 3rd image during movement. After the last image, there was no signal on the detector. All show the nearly same cut-off near column 800.

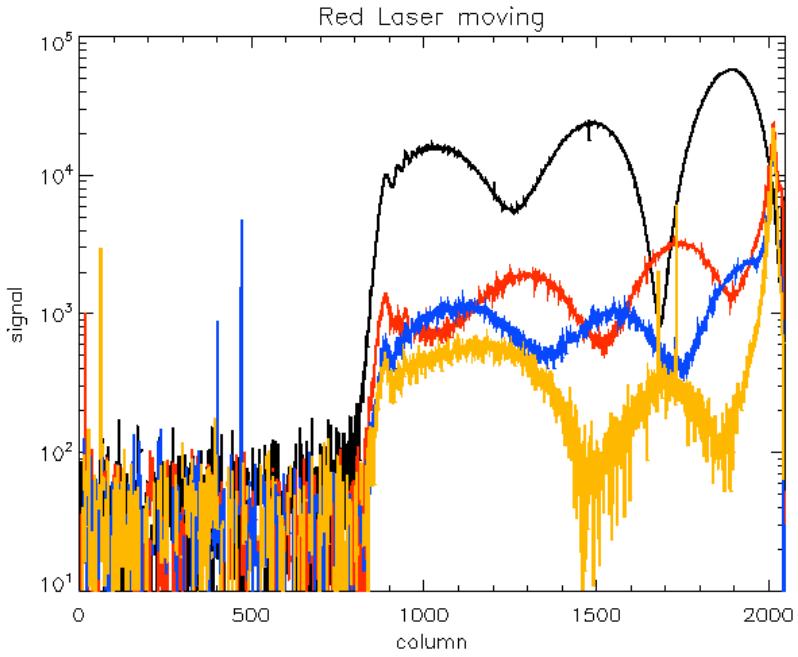

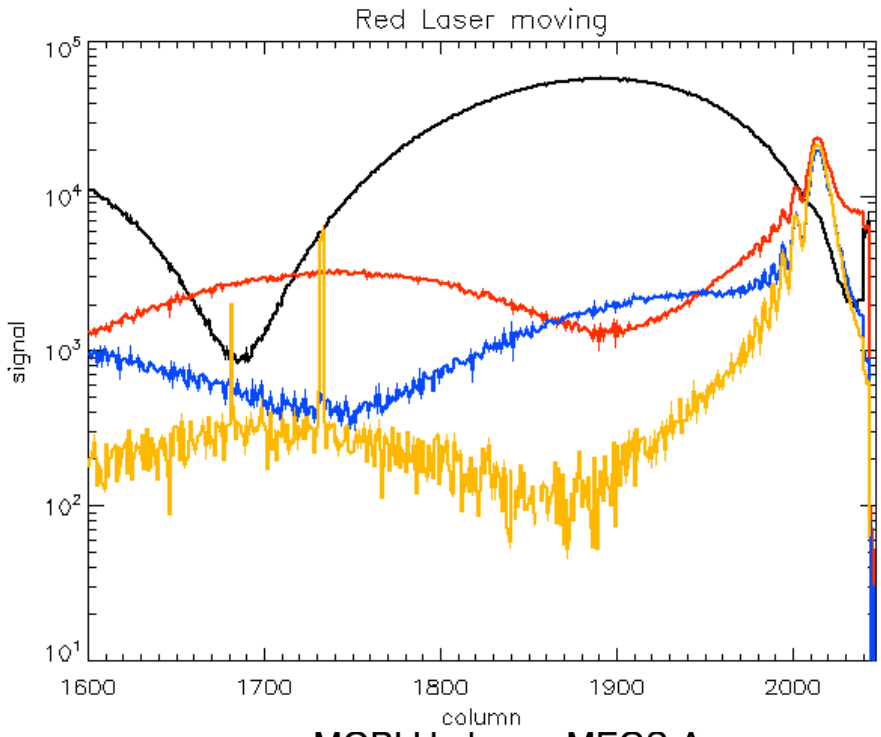
Red Laser moving
signal
column
1600
1700
1800
1900
2000

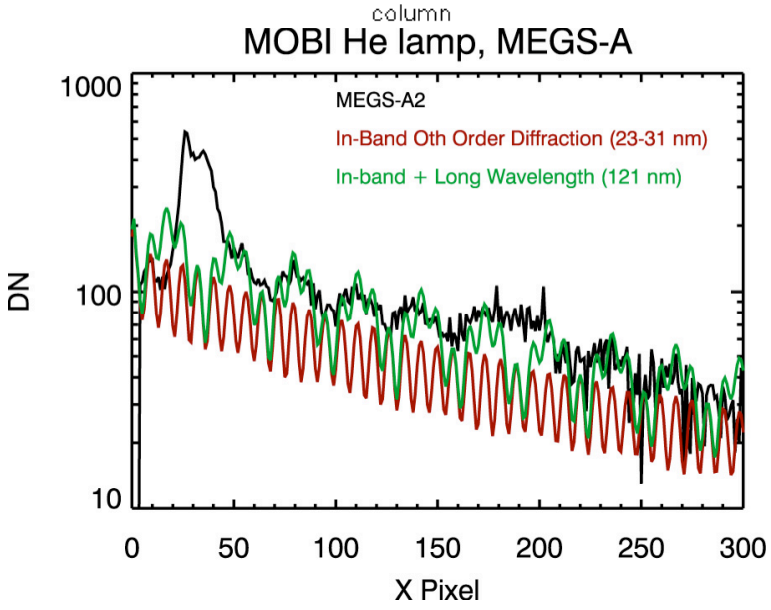
MOBI He lamp, MEGS-A
MEGS-A2
In-Band Oth Order Diffraction (23-31 nm)
In-band + Long Wavelength (121 nm)
DN
X Pixel
1000
100
10
0
50
100
150
200
250
300

10. Quick Responsivity

10.1 MEGS-A

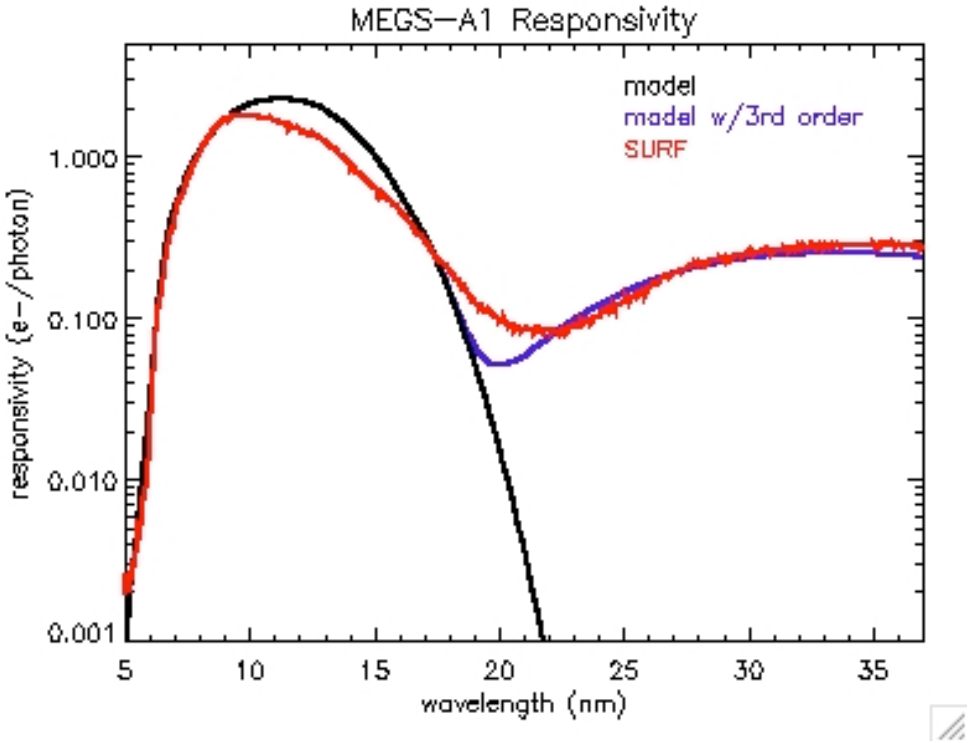

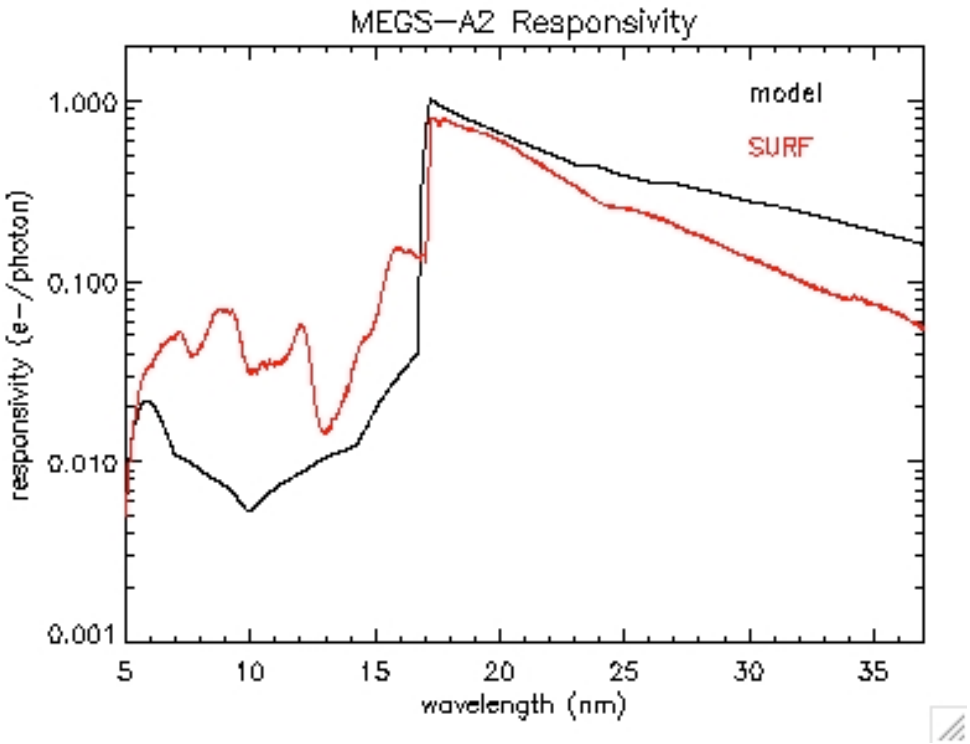

10.2 MEGS-B

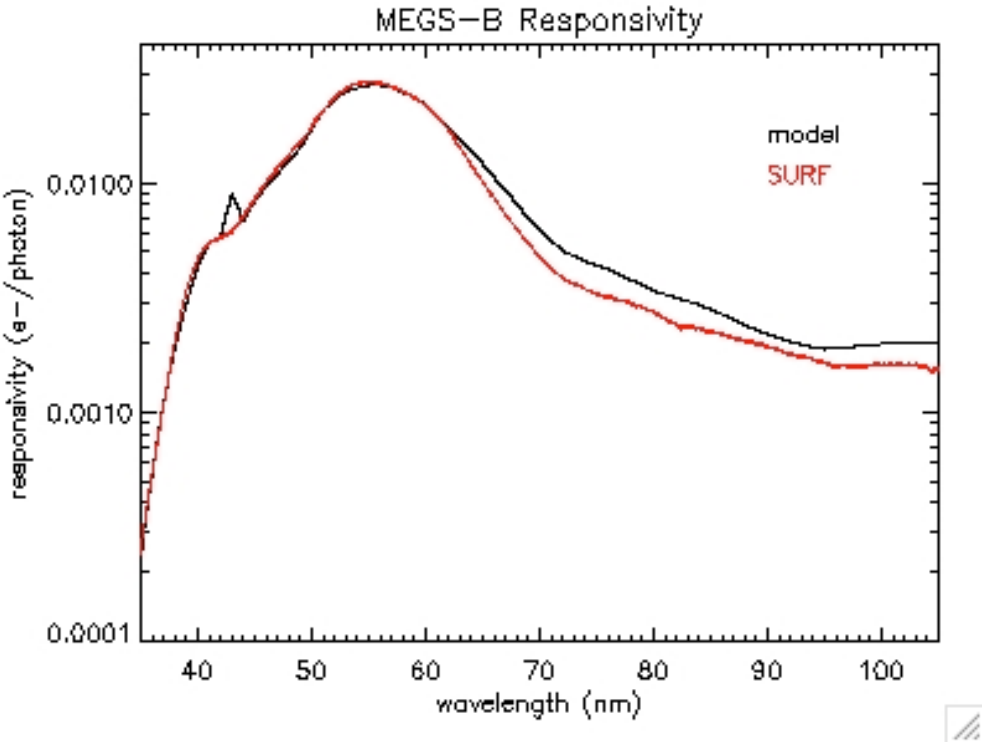

11. MEGS-B Smearing Bottom Right Tap

Use of the bottom right tap for MEGS-B should be avoided. A charge trap is located near the tap that slowly bleeds charge back out creating a smearing effect, or a trail effect like a comet.

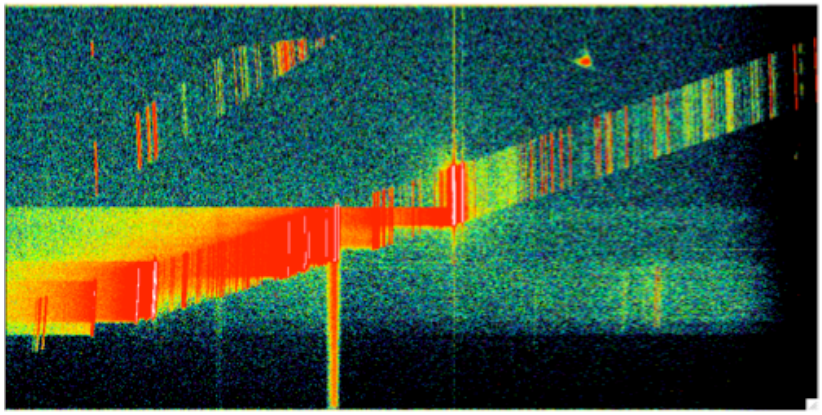

12. Test Patterns (Optical)

Modified text from email conversation with Dave Crotser.

“Below is a CCD image showing the air force test pattern imaged onto device #2 (rocket MEGS-A). Also below is a plot showing x- and y-slices through the image to give you an idea of resolution. This is the image baseline we'll use to characterize CTE for all voltage and FPGA tests. The image was 400x400 pixel area to give you a sense of scale.” This image has been

cropped and resized for presentation.

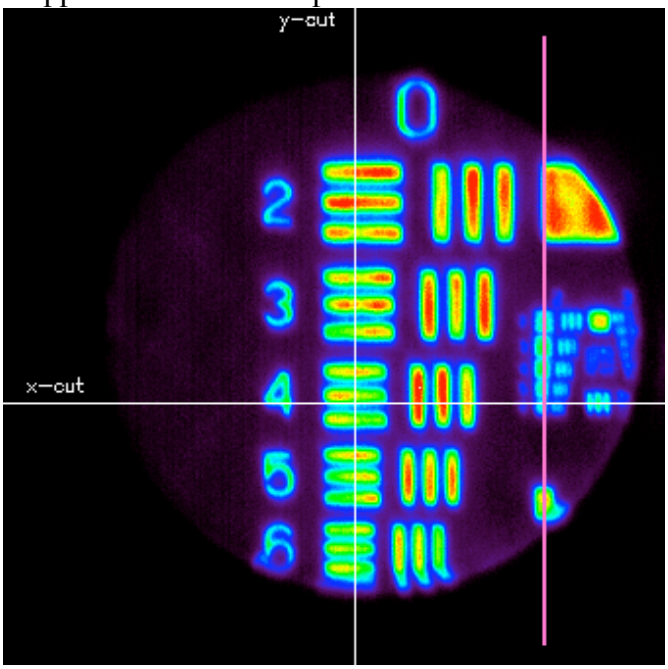

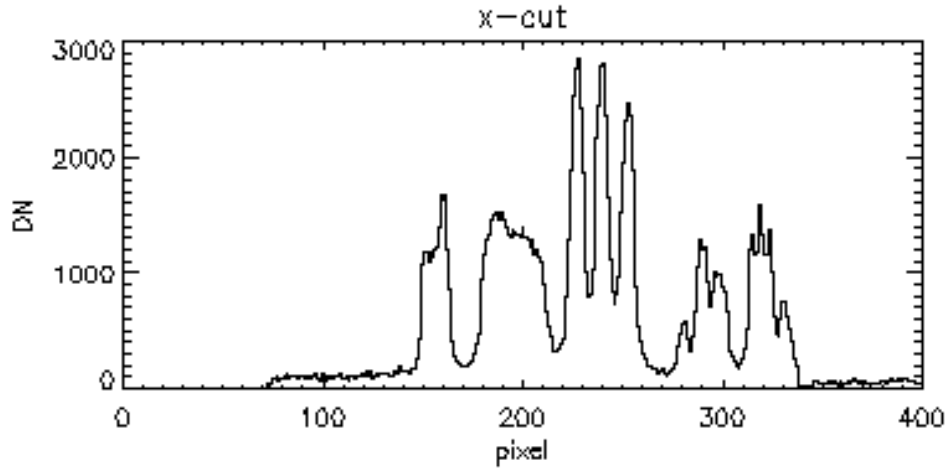

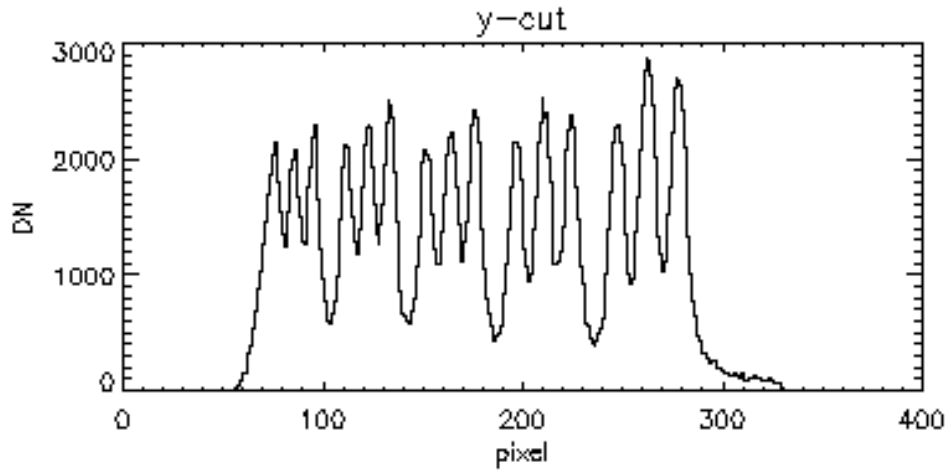

13. Silicon Absorption Depth

Picture provided by MIT 12/06.

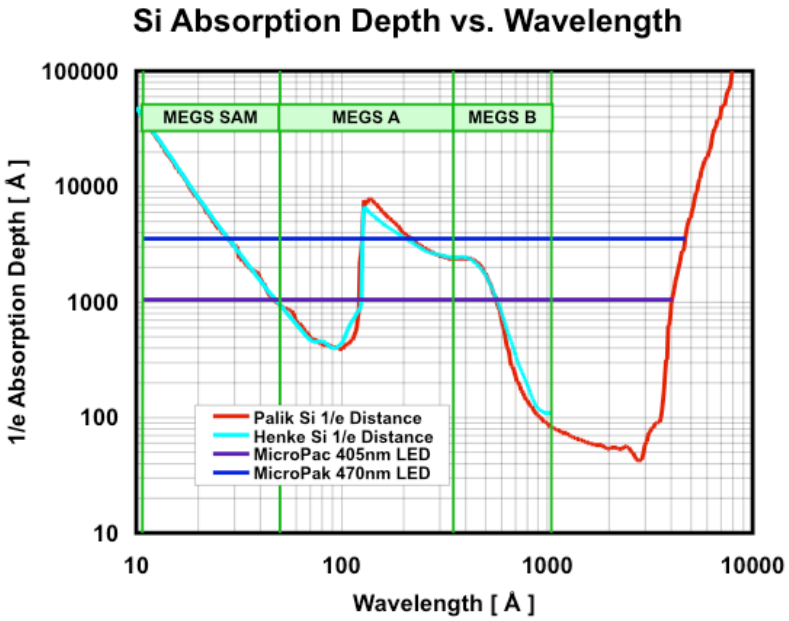

This type of information was used to select the appropriate visible light LEDs used for flatfield tracking in-flight. Selected LEDs were violet (405 nm) and blue (470 nm) shown as horizontal lines in the figure.

Additional green (530 nm), red (640 nm), and infrared (900 nm) LEDs and a Helium line (swept across the CCD) were used to study the striping effect observed on rocket CCDs at different a different clock voltage. This data is compared against the Si penetration depth curve. The small-scale flatfield structure observed in the He line scan appear as dark features indicating less response. All of the LEDs show the features in the same locations; however, they are different because they are brighter (peak-like) features. This is not understood.

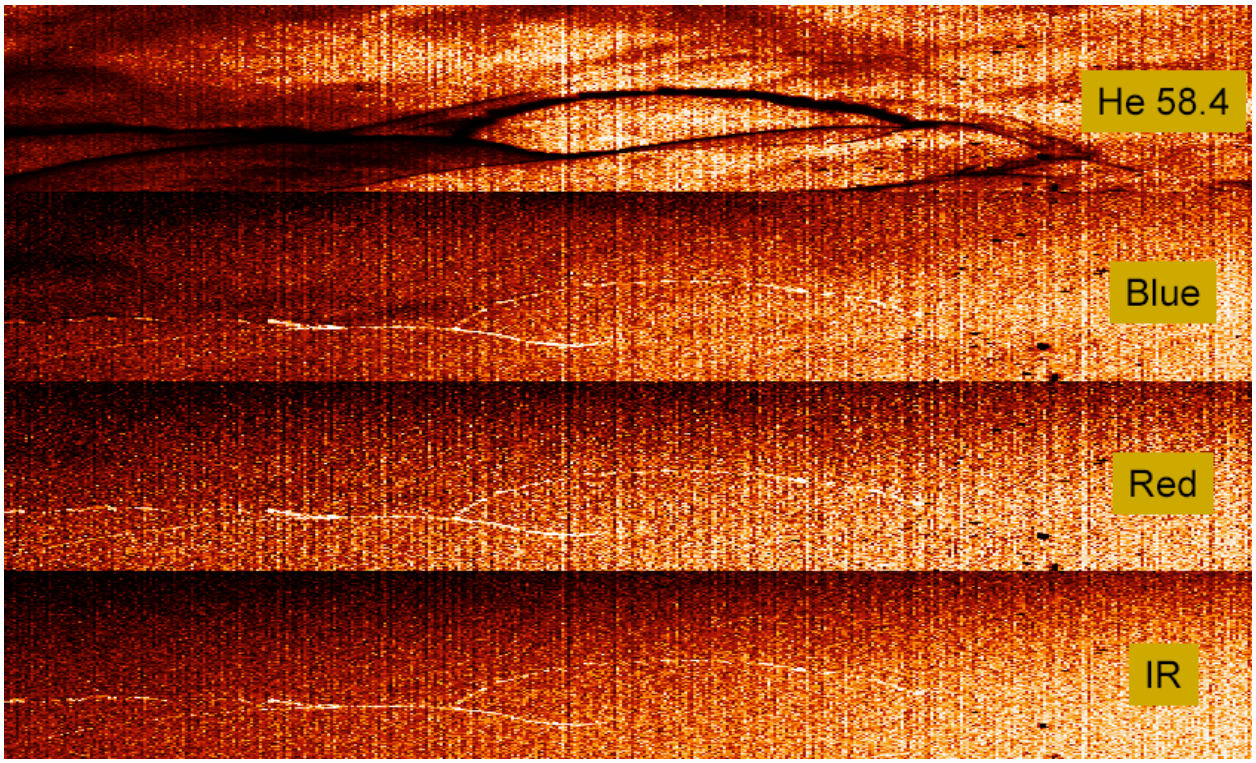

14. Flatfield LED Intensities

During the MOBI alignment and focus testing on March 6, 2007 (day 065), several different LED current settings were used to generate flatfield images. The signals above the background in a 10-second integration are plotted below with the blue and violet LED signals shown as "+" in their respective colors. The dashed lines are linear fits to the available data, and the dotted line represents the threshold needed to achieve 10000 counts over 120 seconds.

Note that these signals are averaged over one million pixels and do not represent the maximum or the minimum signal spread. The illumination shape drops off dramatically near the edges, especially for MEGS-B. Also, these represent the steady-state signals. The signals rise gradually over the first 30-60 seconds.

Based on these line fits, level 5 should be used for MEGS-A blue LED, and level 4 should be used for the MEGS-A violet LED. An LED level of 2 for MEGS-B (for either LED) provides enough statistics to achieve the 10,000 count total. In-flight operational constraints restrict the LED level to be no greater than 9.

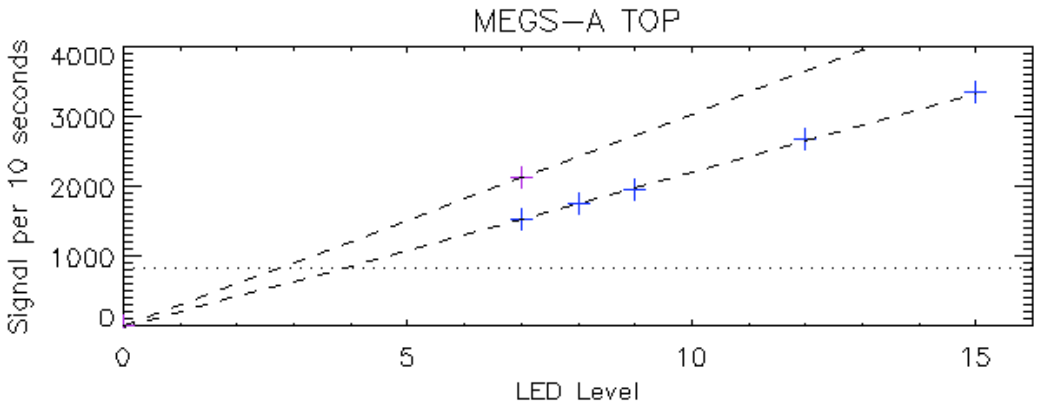
MEGS-A TOP
Signal per 10 seconds
4000
3000
2000
1000
0
0
5
10
15
LED Level

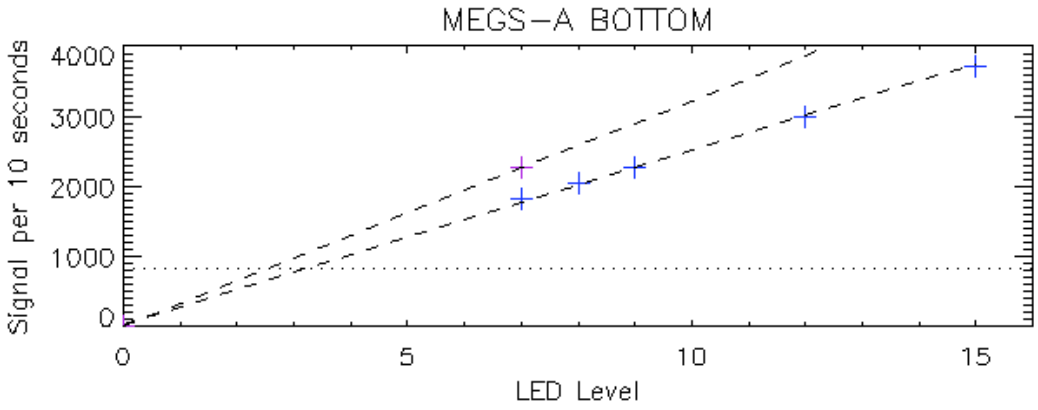
MEGS-A BOTTOM
Signal per 10 seconds
4000
3000
2000
1000
0
0
5
10
15
LED Level

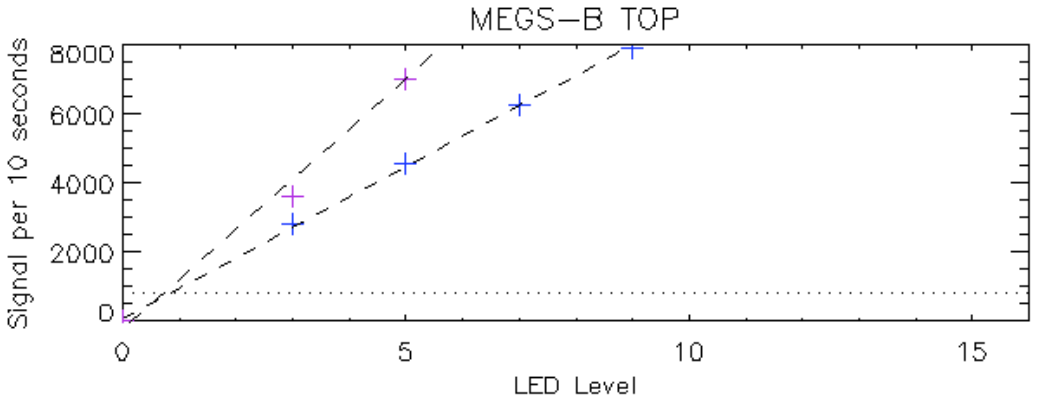
MEGS-B TOP
Signal per 10 seconds
8000
6000
4000
2000
0
0
5
10
15
LED Level

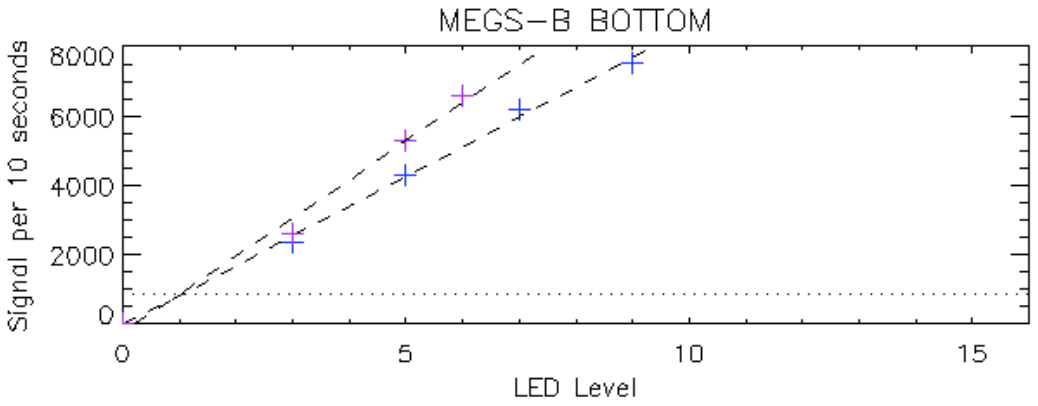
MEGS-B BOTTOM
Signal per 10 seconds
8000
6000
4000
2000
0
0
5
10
15
LED Level